



Enabling the recycling of 3D printed electronics in a circular economy

Master thesis Integrated Product Design
J.H. Nelissen
2018

AUTHOR

Jannes Nelissen

Jannesnelissen@gmail.com

SUPERVISORY TEAM

Chair

Prof. Dr. Ruud Balkenende

Professor Circular Product Design

Department Design Engineering

Section Design for Sustainability

a.r.balkenende@tudelft.nl

Mentor

Dr. Yu Song

Associate Professor Mechatronics Design

Department Design Engineering

Section Mechatronics Design

Y.Song@tudelft.nl

THESIS

Master thesis MSc Integrated Product Design.

Delft University of Technology

Faculty of Industrial Design Engineering

Landbergstraat 15

2628 CE Delft

Delft, April 2018

EXECUTIVE SUMMARY

This thesis describes the research on design measures and new recycling methods to enable the recycling of 3D printed electronics. By looking into methods to release metals from polymer substrate and design interventions to enable predictable fracturing of 3D printed structures in a shredder, a step towards the recycling of valuable metals from future electronics is made.

Recent rapid technological advancements in the production of electronics have created a vast and increasing stream of electronic waste. Not only is this waste a source of toxic pollutants when inappropriately processed, billions worth of valuable metals are squandered as the products are not recycled.

Current technological advancements are made in the development of additive manufacturing techniques that enable the 3D printing of structural electronics. This novel production technique promises enormous possibilities when it is matured as manufacturing method for embedded electronics in consumer products. However, 3D printing of electronics will leave components and circuitry made from valuable metals embedded between fused layers of one or more other materials. This results in the whole piece becoming electronic waste at the product's end of life, with no fitting processes in place to retrieve the value embedded in the product.

Literature research and field studies led to the conclusion that designers should be supported in the design of recyclable 3D printed electronics. Complications in the access to the embedded components and circuitry and liberation of dissimilar materials were identified as main concerns in the recycling process. Explorative studies to solve these two problems were conducted parallelly. One study aimed at the design of 3D printed structures that enable predictable fracturing of the object in a shredder, which facilitates access to the circuit and components in the recycling process. The second study focussed on new methods to achieve the release of silver circuitry from PLA substrate, aiding in the liberation of the this metal in a recycling process.

In the first study several design interventions were found that allow controlled fracturing in a shredder. The best results were obtained with modifications that led to fracture in a horizontal plane, in the direction that the object is build. In the second study promising results were obtained by heating the substrate and circuitry by submerging the object in hot liquid and moving the circuitry and substrate relatively to each other. Ultrasound was investigated as a method to induce this relative movement in the product while it was submerged in hot water. Both methods require further investigation before definitive conclusions can be drawn.

Based on the results of the two studies and a literature study on the current recycling processes for electronics, guidelines for the design of recyclable 3D printed electronics were established. Through a flow chart designers can find the fitting guidelines for their product based on the key characteristics of the product. To enhance and elaborate the formed guidelines, it is recommended to proceed with further research in selected aspects of the studies as presented in the last chapter of this thesis.

TABLE OF CONTENTS

Prologue	II	II Colophon III Executive summary 1 Introduction 1 Reading guide
Foundation Literature and field studies to give direction and lay the groundwork for decisions made in the thesis	02	2 3D printed electronics 3 Circular Economy 4 Preliminary field studies 7 3D printed electronics fit in current recycling processes. 15 Vision
3D print design for liberation The first of two parallel studies. Practical study into the design of 3D printed objects.	16	16 Materials & method 17 Assessment 20 Samples 22 Results 30 Summary of results 31 Discussion 32 Implications for design
Methods to release silver from PLA The second part of the experimental work. An explorative study in methods to release silver circuitry from PLA substrate.	34	34 Methods 35 Method 1: Induction 38 Method 2: Microwaves 40 Method 3: Hot water 42 Method 4: Ultrasounds 43 Discussion of methods and results 44 Implications for design
Guidelines The result of the two experimental studies processed in design guidelines and suggestions for further research.	45	45 Preliminary schematic guidelines for recyclable 3D printed electronic 48 Recommendations for further research
Supplements	51	51 Acknowledgements 52 References 55 Appendix I: Preliminary Field study of non-destructive disassembly 56 Appendix II: Existing guidelines for design for disassembly. 57 Appendix III: Existing guidelines for design for recycling 58 Appendix IV: Preliminary shredder tests. 60 Appendix V: Results design for liberation tests. 62 Appendix VI: Microscope analysis of liberated silver tracks.

INTRODUCTION

3D printing is emerging as a new production technique for electronics. This development conflicts with the advancing realization that we as a society have to change our ways of consumption and production towards a more sustainable circular materials economy.

Due to the nature of the novel manufacturing method, circuitry made from valuable metals and electronic components will be embedded between fused layers of one or more other materials. In contrast to conventional production methods there is no assembly of an electronic system in a separate casing, but instead a whole product, or product part, is fabricated as one integrated piece. This results in the whole piece becoming electronic waste at the product's end of life, with no fitting processes in place to retrieve the value embedded in the product.

The research for this graduation thesis was initiated after the realization that the development of this new production technique will lead to the waste of valuable metals and components embedded in discarded electronics. The goal of the project was to form guidelines for product designers to aid them in the design of 3D-printed electronics that will fit a circular economy.

Reading guide

To determine in what way the production technique should fit the circular economy, what the opportunities and limitations are, literature research was done into the development of 3D printing of electronics and the circular economy.

Based on the literature, three preliminary field studies were conducted to determine the direction of the project. It was concluded that recycling of the embedded circuitry should be the aim of the project.

A literature study into current recycling methods for electronics was done to identify the main barriers in the recycling of 3D printed electronics with conventional methods with regards to design requirements.

Following the literature and preliminary field studies a vision was formed for the course and goal of the research. Two main concerns needed to be addressed: Accessibility of the circuit and enabling release of the metal from the substrate.

The explorative studies into design for liberation and methods to release silver from PLA are conducted in parallel and the implications of the results on the design guidelines are interdependently influenced.

The result is a set of design guidelines for 3D printed electronics that will aid to improve the recyclability of embedded metals. A designer is guided to the right guidelines by a flow diagram based on the characteristics of the product to be designed.

The results from the explorative studies raise questions that can lead to further research.



Figure 1: Illustration of the structure of this thesis.

3D PRINTED ELECTRONICS

A literature study was conducted into the performed research on 3D printing of electronics to analyse how this production technique is developing and to determine whether there are any shared characteristics between the electronics manufactured through 3D printing. This can be used to guide the direction of the research and to identify challenges later in the project.

Development of 3D printed electronics

Since the late 1980's several forms of additive manufacturing methods have been established (Wohlers & Gornet, 2014). These include the more commonly known stereo-lithography and fused deposition modelling, also known as 3D printing, which are widespread in use as manufacturing methods for both prototyping and end-use final products.

Over the past decade 2D printing with electronic conductive materials has been established as production method for small electronic components, through both conventional screen printing and offset printing and more recently inkjet and aerosol printing, with the production of RFID tags as most common example (Kantola et al, 2009). New research has now led to the development of additive manufacturing with conductive materials in three dimensions. This production technique shows great advantages during the prototyping of structural electronics (MacDonald et al, 2014) and promises enormous possibilities when it is matured as manufacturing method for embedded electronics in consumer products (Ota et al, 2016).

Production characteristics

Currently 3D printing with embedded electronics is still being developed and mainly used for experimental purposes. Methods of production vary per study, shared characteristics are that the chosen substrate is made from a polymer and built up by consecutive added layers with the addition of three dimensional circuitry that is not limited to the conventional planes. Electronic components are placed in voids that are left in the printed shape, and can only be placed when the shape is printed as high as the highest point of the to be placed component (Hoerber et al, 2014). Circuitry is made with conductive polymer inks (Sanatgar, Campagne & Nierstrasz, 2017), aerosol jetted silver inks (MacDonald & Wicker, 2016), drawn wires (Espalin et al, 2014), cured liquid inks (MacDonald et al, 2014), microchannels with liquid conductors (Ota et al, 2016), or conductive pastas (Wu, Yang, Hsu, & Lin, 2015).

As a production technique 3D printing is relatively slow compared to conventional methods such as injection moulding or thermoforming (Gao et al, 2015). Embedding electronics adds to this production time and with the current state of the technology, the costs of conductive inks amount to a much higher cost per piece in production when compared to prevailing production methods (MacDonald et al, 2014; Bailey, Stoyanov, Tilford, & Tourloukis, 2017). The 3D printing technique

does have its unique benefits over conventional methods of production for both the electronic circuitry and components and the casing of the electronics. These benefits are the ease of customization, form freedom in circuitry (MacDonald et al., 2014), and the opportunities for miniaturization of components (Sun et al., 2013) and integration of electronic systems in products (Wu, Yang, Hsu, & Lin, 2015).

Examples of applications

Current research and literature supply examples of future applications in which the advantages of 3D printed electronics can be used:

- Personalized consumer electronics such as smart wearables (Gao et al, 2015;)
- Embedded sensors in medical products such as casts and prostheses (Ota et al, 2016).
- Small test batches and prototypes of electrical devices that eventually will be made with other methods for final production (figure 2). (MacDonald et al, 2014)
- 3D shaped electromagnetic coils for better fitting in a product, for example: antennas, induction coils, or embedded electromagnets. (MacDonald & Wicker, 2016)
- 3D placement of conventional (2D) electronic components on a 3D circuit for weight and space optimization. For example in robotics and aerospace applications, in and on housing that does not need to be 3D printed. (Wu et al, 2015)
- 3D printing of electronic components in unconventional shapes. The technique releases them from boundaries in shape set by conventional production methods. For example printed circuit boards (PCB's) and batteries that require a better fit or advanced miniaturization, also to be used in other products that do not necessarily need to be 3D printed. (Gao et al, 2015; Malone & Lipson, 2008)



figure 2: prototype of a electronic gaming dice with embedded accelerometer, microprocessor, and LED's. (MacDonald et al.,2014)

CIRCULAR ECONOMY

To identify how 3D printing can be fitted in a circular economy, a literature study was conducted into the necessity to establish a circular economy and the principles behind it.

Electronic waste in the linear economy

Our current economy is dominated by a linear 'take-make-use-dispose' model. Production and consumption in this model rely heavily on the supply of raw materials, are based on inefficient use of energy and cause unnecessary waste and releases of CO₂ in the environment (Ellen MacArthur Foundation, 2013a). One of the major consequences of our linear economy and rapid technical innovation is electronic waste (e-waste) (Baldé et al, 2015). Not only is this e-waste one of the most toxic pollutants in the municipal waste stream (Ongondo et al, 2011), it is a waste of residual value stored in the electrical components and materials (Ellen MacArthur Foundation, 2013b). In a study for the United Nations it was found that 44,7 million metric tonnes ($44,7 \cdot 10^9$ kg) of e-waste was generated in 2016, rising 8% since 2014, with a total value of 55 billion euros in raw materials of which only 20% was recycled (Baldé et al, 2017).

Circular Economy as sustainable economic model

The Circular Economy is an alternative economic model based on continuous cycles of recovering and reuse of products, parts, and materials, with as goal to minimize environmental impact and to optimize the recovery of value embedded in products and materials. In a Circular Economy products are designed for maintenance, reuse, refurbishment, remanufacture and/or recycling (Ellen MacArthur Foundation, 2013a&b). These cycles are depicted as the blue loops in the Circular Economy model shown in figure 3.

The more inward the loop is, the more value is retained in the product or part. Each loop outward will require more investments in terms of material, energy, and labour, and create more waste and emission of harmful substances.

Ideally the products are kept in use as long as possible and cycled through the inner three loops, as these are non-destructive processes in which previously added investments to the parts are retained. Recycling is the most outer loop and is a destructive process in which the product is destroyed to reclaim its materials.

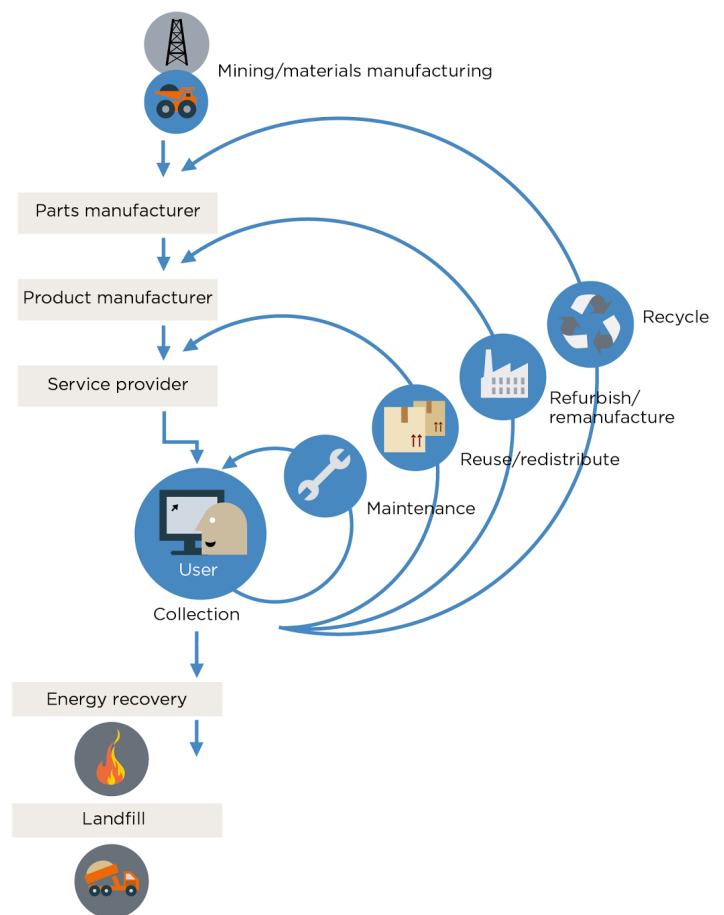


Figure 3: Model of the circular economy (adapted from Ellen Macarthur Foundation, 2013a)

PRELIMINARY FIELD STUDIES

To determine the goal of this thesis three preliminary studies were performed. As described in the previous chapter, 3D printed electronics can fit a circular economy in several ways; for instance by enabling the maintenance or repair of the functional parts of the products to prolong the lifespan, or by enabling recycling of the materials where the product is comprised of. These small field studies were conducted to find how 3D printed electronics can fit in a circular economy the best and to find hiatus in the existing design guidelines. The conclusions are summarized in this chapter, the studies are discussed in further detail in appendices I to IV.

Design guidelines

The first study was a literature review of design guidelines, to determine to what extent the guidelines for the design of conventional electronics inform on how 3D printed electronics can be designed to better fit disassembly or recycling processes. These guidelines can be found in appendices II & III. It was found that these guidelines for conventional products are largely not applicable to 3D printed products. No design guidelines were found that specify design interventions that will help to improve the recyclability or disassembly of 3D printed electronics specifically.

Design for disassembly

In the second preliminary investigation 3D printed objects were designed and built with modifications that allow for non-destructive disassembly in order to access parts of an object and in some cases reassembly of the object. Products that can be repaired or upgraded will retain more value in their lifecycles, as described in the previous chapter. This small study was conducted to see how design interventions to enable non-destructive disassembly affect other aspects of the products.

Figure 4 shows one of the 3D printed models, a more elaborate description of this study can be found in appendix I. It was found that incorporation of these measures require adjustments in the object that conflict with some of the core benefits of 3D printing as a production technique for the manufacturing of electronics, as summarized in table 1.

Shredding

In the third and last preliminary study, an experiment was performed in which samples of 3D printed electronics were shredded in a cutting mill. This was done to see whether the recycling of the 3D printed electronics would indeed pose problems with the liberation as expected at the start of this project.

During the experiment three sieves with different sized holes were used in the shredder, varying the resulting size of the produced shreds. Further explanation of the experiment and the results can be found in appendix IV. From the experiment it was concluded that even with the smallest sized shreds possible in this experiment, the liberation of silver circuitry from the sample's substrate was insufficient to be appropriate for a circular economy. Table 2 shows the weight percentage of middlings, shreds with a combination of dissimilar materials (see figure 5), in the fraction with liberated and separated silver shreds.

Following from these results of the preliminary studies it can be concluded that a research into the possibilities for improvement of recyclability of 3D printed electronics is justified.

non-destructive disassembly	Benefits 3D printed electronics
System build in subassemblies	Better integration of electronics
Needs space for structures.	Miniaturization
Needs space for dis- and reassembly.	

Table 1: conflicts between requirements and benefits of design for disassembly and 3D printing electronics

Maximal shred size →	< 8 mm	< 6 mm	< 4 mm
% middlings in silver containing fractions	65,0	61,5	37,5

Table 2: percentage of middlings in the silver containing fraction per sieve size.



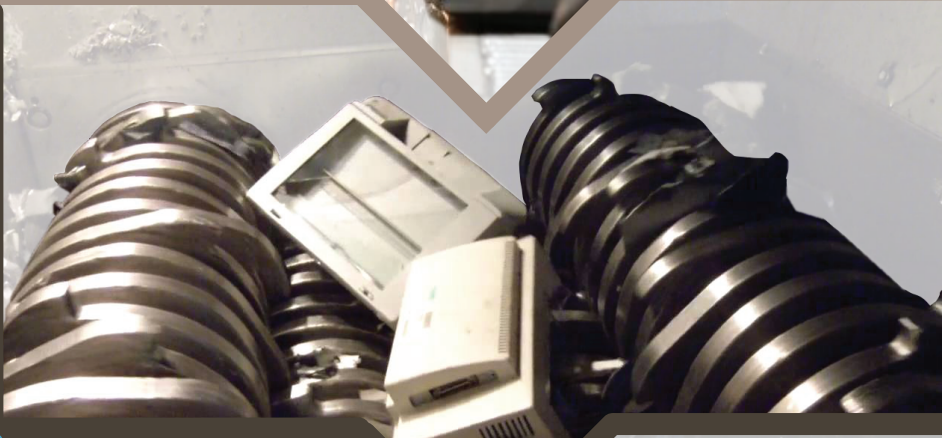
figure 4: a 3D printed casing for a bike light with covers that can be printed over to seal the product, but can be broken open to retrieve the parts. Part of the preliminary field study into design for non-destructive disassembly.



figure 5: fractions of middlings: shreds with a combination of dissimilar materials. Part of the preliminary field study into release of the silver from PLA substrate in a shredder.



Disassembly



Liberation



Sorting



Purification

figure 6: illustration of the four stages of the recycling process.

3D PRINTED ELECTRONICS FIT IN CURRENT RECYCLING PROCESSES.

This chapter discusses the current practice of recycling of electronics and how these processes match the distinctive aspects of 3D printed electronics. From this review can be surmised what obstacles need to be overcome by design interventions to improve the recycling of 3D printed electronics.

Generally consumer and non-consumer electronics are recycled as described in this chapter, this includes home appliances such as televisions and refrigerators, but also office and telecom devices such as desktop computers, printers, and mobile phones, and even electronic road signs, defibrillators, security camera's, and network servers. Recycling for such products can be regarded as a four stage process, in which materials are taken from products or parts to a refined material that can be sold to producers, with the following steps (Kumar, Holuszko, and Espinosa, 2017):

- Dismantling
- Liberation
- Sorting
- Purification

Dismantling

During the dismantling parts with high concentrations of precious metals, reusable components, and toxic parts are removed from the product before it is shredded. Regulations on the production and disposal of electronics (EU directive on WEEE, 2012) require selective treatment for certain components in consumer electronics, for instance removal of batteries, lighting elements containing mercury, and LCD's (of a minimal size) to prevent their hazardous substances from spreading during shredding (Kumar, Holuszko, Espinosa, 2017). Other components are taken out during dismantling to be recycled further in a specially designed process for their precious materials. PCB's for instance, which have valuable metals concentrated on a small surface and can be recycled more efficiently when treated separately (Li, Lu, Xu, Zhou, 2007).

Liberation

To liberate the various materials used in a product or part from each other for further processing, the products need to be shredded into small particles. There are numerous ways of reducing a product into smaller bits, including milling, cutting, grinding, abrasion, and crushing (Kaya, 2016). The usual method is a combination of these ways in a machine with heavy blades that rotate around two opposing axis, crushing and cutting what falls between them. The shreds vary in size depending on the methods of separation and purification that follow. Cui and Forssberg (2003) wrote the following about PC and PCB scrap: "industry scale tests showed that after two stages comminution, the liberation of -5mm fraction is between 96.5 and 99.5%"

In the design of 3D printed electronics the dismantling stage can be taken into account by making the valuable and hazardous components easily accessible and retrievable with standard manual tools. Complications can be foreseen due to the fact that components will be embedded between fused substrate layers. Furthermore 3D printing the electronics will lead to spreading of both the circuit and components over the product, instead of having them concentrated on a PCB for instance.

In the design of 3D printed electronics the use of shredding when recycling can be taken into account by making the material that is to be recycled is releasable in a shredder. This design intervention is referred to as "Design for Liberation" and usual features are split lines, stiff connections, and avoidance of ductile materials in the casing of electronics. The test with the release of silver off the substrate (see appendix IV) indicates that shredding to a common particle size of 5mm is not enough for liberation, further complications are likely to arise when the circuitry is embedded between substrate layers.

Sorting

Due to the diversity in materials used in modern electronics, a wide variety in separation methods exist to sort the shreds after comminution. The sorting methods are described in further detail because they set requirements to the feed stock of shreds in terms of size and composition, this might set requirements to the shredding and pre-processing and to the design of the products.

Weight and density

Most electronic scrap consists of a mix of plastics (ABS, PC, PPE, HIPS), light metals (aluminium), and high density metals (copper, ferrous metals, and silver, gold, and platinum in smaller amounts) (Basha, 2007; Kaya, 2016; Wäger & Hirschier, 2017). The differences in density between these fractions enables separation based on gravity by various methods such vibrating tables or wind sifters, these methods do require scraps with nearly constant volumes (Cui and Forsberg, 2003).

Other methods that capitalize on the difference in density rather than weight are float-sinks and gas or hydro cyclones. Fifteen years ago it was already reported that these later centrifugal methods can achieve 97% copper recovery in the recycling of PCB's when combined with the right pulverising processes (Goosey and Kellner, 2002).

Several sources write that these density based methods are mainly used to separate the metal fractions from the non-metal fractions, with other separation techniques to sort the different metals from each other (Cui and Forsberg, 2003; Li et al., 2004; Kaya, 2016; Kumar et al., 2017).

Commonly for the separation of plastic and PCB scraps from metals, sink-floats with a medium with a density of 2,0 g/cm³ are used (Kaya, 2016). PLA has a density of 1,24 g/cm³ (NatureWorks, 2016) and silver 10,49 g/cm³ (WolframAlpha Knowledgebase, 2018).

The theoretical minimal volumetric percentage can be calculated:

$$\text{Volumetric\%} = \frac{(\rho_{\text{medium}} - \rho_{\text{PLA}}) / \rho_{\text{Ag}}}{1 + ((\rho_{\text{medium}} - \rho_{\text{PLA}}) / \rho_{\text{Ag}})} = 6,8\%$$

The surface area of the cross section of a silver track is 0,4*0,25 mm = 0,1 mm² (Maas, 2017). This leads to a maximal surface area of the cross section of PLA of 0,1/0,068= 1,48 mm².

It can be concluded that the maximum size of shreds with unliberated silver tracks on them should be $\sqrt{1,48}$ = 1,22 mm in diameter

box 1: calculation of maximal shred size of middlings in density separation

Purity is defined as the percentage of the desired material versus undesired contaminants in a separated fraction.

Recovery indicates the amount of the desired material that is recovered in the fraction as a percentage of the total amount of that material in the original product.

box 2: Explanation of the difference between the terms purity and recovery.

In the recycling of 3D printed electronics the use of weight separation is difficult as scrap with nearly constant volumes is needed, requiring the whole product to be shredded as small as the thin silver traces. Density separation can be used, as the significant difference in weight between the metal and substrate, but it does require liberation of the metals from the substrate in a previous stage. Incorporation of various metals will require a combination with another separation technique. Incomplete liberation of the small traces will either result in the loss of silver or impurities in the recovered silver, see the calculation on the maximum shred size for middlings in the box 1.

Magnetic

A broad spectrum of magnetic separation methods exists with distinctions that range from low to high volume processing, wet or dry processing, and small to big particle separation (Svoboda & Fujita, 2003). For the recycling of consumer electronics a method of dry high intensity separation is used. A mix of particles is fed over a rotating magnetic barrel. Non-magnetic particles will not adhere to the barrel and will be separated from the magnetic fraction that sticks to the barrel. The magnetic fraction releases from the barrel due to centrifugal forces and gravity, see figure 7. In some cases the difference between the magnetic forces of different materials is used to further separate strong and weak magnetic fractions. However, the main application (of dry high-intensity processing) is the recovery of ferromagnetic metals from non-ferrous metals and non-magnetic waste (Veit et al, 2005). The particle size does not affect the efficiency of the separation, as the size influences the gravity as much as it influences the magnetic force.

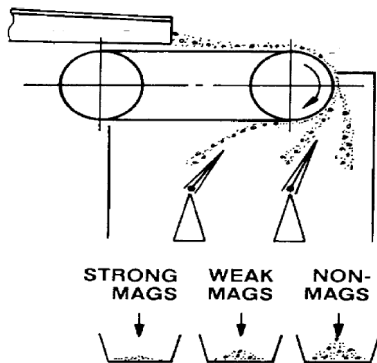


Figure 7: Magnetic separation (Svoboda & Fujita, 2003)

Electrostatic separation

Electrostatic separation resembles the magnetic separation methods visually, but is based on the difference in conductivity of different materials and is mainly used to separate metals from non-metals. Shredded particles are dropped on a downward rotating barrel, which is conductive and grounded, close to this barrel is an electrode that ionizes the particles. Non-conducting material will become statically charged and stick to the barrel while it rotates until it is brushed off at the bottom of the barrel, where all non-conductive particles are collected. Particles from conductive material, however, will discharge through the barrel and will fall from the barrel, or will be “shot” off due to the centrifugal and friction force, and will be separately collected from the non-conductive materials (Veit et al, 2005).

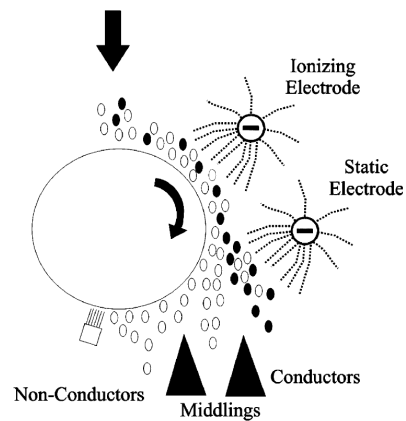


Figure 8: Electrostatic separator (Veit et al, 2004)

This separation method is a low capacity process because it requires a feed of a small layer of particles to the barrel, with fine particles smaller than 0,6mm (Wu, Li & Xu, 2008). Guo et al (2011) even conclude that a particle size between 0,15 and 0,3 millimetre is optimal for both the recovery and purity of the metal fraction (box 2 explains the difference between these two terms). Particles of combined conductive and non-conductive materials that are not well separated (“middlings”) can cause impurities in the separated fractions as the composition will determine the balance between the Coulomb force and the gravity and thus where the particle will fall from the barrel.

In the recycling of 3D printed electronics the use of magnetic separation is limited to the separation of ferrous metals, for for instance embedded components, from the rest of the fraction.

In the recycling of 3D printed electronics the use of electrostatic separation is complicated. The low volume process conflicts with the spread of the small volume percentage of the metal fraction over the big volume of the printed substrate.

Eddy current separation

Eddy current separation is another method based on the conductivity of materials, but it also depends on the density of the materials. Non-ferrous particles will be fed over a conveyor belt with a rotating roll of alternating oriented magnets at the end. This roll causes a changing magnetic field that in turn causes magnetic fields in all the conductive particles in the fraction. A Lorentz force is created as a reaction between the magnetic field of the rotor and the magnetic field in a particle, this deflects the particle away from the rotor, see figure 8.

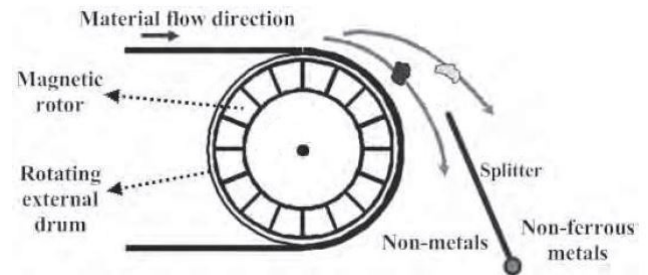


Figure 8: Eddy current separator (Yazici, Deveci, Alp, 2010)

Because different materials vary in conductivity and have a unique density, the fed material can be sorted in fractions per metal by the distance that they are deflected away from the magnetic rotor, provided that they are of equal size and shape. This unique combination of properties per material is called the deflection coefficient, noted as σ/ρ (Yazici, Deveci, and Alp, 2010). Table 3 shows the deflection coefficient of common materials found in electronics. The bigger the contrast between the coefficients of the various materials in a feed fraction, the higher the purity of the resulting fractions becomes.

As mentioned, both homogeneous particle composition and a near uniform particle size is important, as increased particle size will result in an increased Lorentz force, affecting the deflection. A feed of consistently larger sized particles will result in a bigger contrast in deflections, thus better separation between fractions (Zhang et al, 1998). Zhang, Rem and Forssberg (1999) reported that rectangular, sheet-like particles will be better deflected than sphere shaped particles. From this can be concluded that for better separation (higher purities) a feed of uniformly shaped particles is preferred. Reported numbers regarding the optimal size of the granulated feed vary. Both Cui & Forssberg (2013) and Lungu (2009) note 5 mm as minimal workable particle size, Zhang et al (1998) reported a range of 2-7 mm as optimal for a high recoveries rates with the highest purities.

Non-conductive materials will not be affected by the magnetic field and will fall from the conveyor belt. Ferrous metals will heat up in the eddy current field (through magnetic hysteresis losses), this can lead to damages to the conveyor belt. Thus, the presence of ferrous metals in the fraction that is fed to the eddy current separator must be prevented.

Material	Deflection coefficient, σ/ρ ($10^3 \cdot M^2/\Omega \cdot kg$)
Aluminium	13,0
Copper	6,7
Silver	6,0
Zinc	2,4
Gold	2,1
Tin	1,2
Lead	0,45
Plastics	0

Table 3: Deflection coefficient of some common materials found in WEEE recycling fractions. (Yazici & Deveci, 2009)

In the recycling of 3D printed electronics, the method of eddy current separations seems inapplicable. The requirements of a near uniform particle size as well as a minimal work size of 5 mm do not match the tests results (see appendix IV) that show that the silver is not liberated from the substrate when shredded at this size.

Purification

The final fractions that result from the mechanical separation processes are chemically treated to be purified to materials that can be sold to be reused for production. This is mostly used to recover and purify copper, gold, silver, and palladium (Kumar et al, 2017). The most widely used processes are pyrometallurgy and hydrometallurgy, and more recently extensive research has been done into bio-metallurgy (Namias, 2013; Kaya, 2016; Zhang & Xu, 2016).

Bio-metallurgy

Bio-metallurgy fits best with the circular economy principles as it is an environmentally friendly process in which microbes are used to leach specific metals out of the fractions. This is a promising technique that is currently in development to be used for the recycling of metals, but is not economically viable on industrial scale (Yang et al, 2014; Zhang & Xu, 2016). It is already commercially used for metal extraction from sulphide ores in the mining of gold and copper (Namias, 2013). The microbes are used to create acids that dissolve the metals in water, the metal atoms are singled out and extracted through electro-winning (Zhang & Xu, 2016).

Pyrometallurgy

Pyrometallurgy is the most common method of recovery and purification of metals. "The main advantage of pyrometallurgical treatment is its ability to accept any forms of scrap" as Kaya (2016) puts it, and the fast reaction rates (Kumar et al, 2017). This means that mixed metal fractions that are not further mechanically separated are processed together. In some facilities PCB's and small electronics are not even shredded but directly sent to smelters (Namias, 2013; Buchert et al, 2012). Currently the main goal, based on economical grounds, of this form of purification is to recover copper and gold. Copper because it accounts for the highest content in the metal fraction of waste PCB's, and gold because it accounts for the highest value in the fraction (Yu et al, 2009, as cited in Akcil et al, 2015). Other valuable metals such as silver, platinum, or palladium can be recovered too in a pyrometallurgical route, while metals such as tin and zinc will compound to flue dusts or slag which can be further refined in hydrometallurgical processes but this is limited by economic efficiency (Reuter et al, 2013).

First the fractions are melted at high temperatures with copper concentrate, the metals are divided in a mix of copper with smaller amounts of noble metals (Au, Ag, Pt, Pd), and a slag containing the other metals (Al, Fe, Pb, etc). Pure copper is extracted from the copper solution in an electrorefining process. Depending on the composition of the rest of the precious metals bullion, further refining processes are applied, usually through electrorefining too.

The use of bio-metallurgy is not yet applicable in the recycling of 3D printed electronics, for this project specifically, because no method to recover silver is found and in general because it is not yet economically viable on an industrial scale.

The use of pyrometallurgy is applicable in the recycling of 3D printed electronics. Small electronics with a sufficient metal to substrate ratio can be sent to the smelter integrally, for bigger products the spread of circuitry and components throughout the product will require a form of concentration of the metal fraction. Disassembly is needed for products containing hazardous substances, or for the refinement of non-compatible metals such as aluminium.

Hydrometallurgy

Hydrometallurgy is a more selective refining process, in which specific metals (from a concentrated pre-sorted solid fraction) are dissolved in chemicals to be separately purified and recovered. For the recovery of precious metals (such as silver in this research) hydrometallurgy is preferred over pyrometallurgy (Cui & Zhang, 2008, as cited by Akcil et al, 2015). This is because of the higher recovery rate of these metals (Akcil et al, 2015), it is easier to control the reaction, and creates less environmental hazards (Kaya, 2016), and lower energy demand (Kumar et al, 2017).

For successful recovery the waste needs to be granulated and mechanically sorted to a concentrated mix of non-ferrous metals (Lu & Xu, 2016), For a high metal yield the granulate should be of small grain size (Gramatyka, Nowosielski, and Sakiewicz, 2007). The granulate goes through a series of acids or other corrosive substances that each dissolve specific metals from the solid granulate, these solutions are concentrated to contain the desired metals and separate impurities (Namias, 2013). Recovery of the metals from the leachate (solutions) is done via electrowinning, solvent extraction, and precipitation (Namias, 2013; Kaya, 2016). For silver the most common and currently economically most feasible method for leaching is with cyanide (Namias, 2013; Akcil et al, 2015; Lu & Xu, 2016), and recovery through electrowinning. The obvious drawback of cyanide as a solvent is the high toxicity and the fact that the use generates large amounts of (toxic) waste water (Lu & Xu, 2016). Currently promising research is done to find substitutes that have proven to be successful in laboratory setting such as thiourrea (Cui & Zhang, 2008, as cited in Namias, 2013), iodine (Lu & Xu, 2016), and sulphuric acid (Akcil et al, 2015).

Summarizing conclusions

A summary of this review of the conventional process of recycling of electronics and how this matches with a possible recycling of 3D printed electronics can be found in table 4. In the table a distinction is made between the recycling of 3D printed electronics in the form of the available samples used for this project (discussed on page 15), and recycling of possible future 3D printed electronics manufactured and recycled on industrial scale.

The use of hydrometallurgy is applicable in the recycling of 3D printed electronics. The requirements set by this method are that the metals are exposed and for a high yield need to be granulated to a small size. For efficient treatment, concentration of the metal fraction in the granulate is required.

Step	Current Samples	Future 3D printed electronics
Liberation		
Dismantling	No dismantling is needed. The current manufactured samples have exposed circuits and no embedded components.	Components and circuit will be spread throughout a product instead of concentrated on a PCB. 3D printed electronics with embedded components will require a method to be selectively opened for the removal of components.
Shredding	Tests (appendix IV) show that 3D printed silver does not fully release from the PLA substrate at shred sizes of 8, 6, and 4 mm.	Circuits and components will be embedded between printed substrate layers, further complicating the release of materials.
Sorting		
Density	Applicable. Middlings of silver stuck to shreds of substrate require a trade-off between recovery and purity.	Applicable. But embedded circuit and incorporation of various metals further complicate density separation. Improper liberation of dissimilar materials requires small shred size.
Magnetic	Not applicable as the samples do not contain ferrous metals.	Only applicable to separate ferrous fraction.
Electrostatic	Complicated due to small volume percentage of silver on substrate. Middlings cause problems.	Not applicable. This is a low capacity process, which does not match with the spread of components and circuit through the product instead of concentrated on a PCB.
Eddy Current	Not applicable. A near uniform particle size is required as well as a minimal work size of 5 mm. Tests (appendix IV) show that the silver is not liberated from the substrate when shredded at this size.	
Purification		
Bio metallurgy	Not applicable to recover silver.	Not economically viable on industrial scale.
Hydrometallurgy	Applicable. A fine grain size is required for high yield.	Applicable. Does require exposed circuit. A fine grain size is required for high yield, which in turn requires a preceding mechanical concentration (through density separation for instance).
Pyrometallurgy	Applicable	Applicable. Small electronics can be sent to the smelter integrally. For efficient treatment of metals in non-concentrated fraction, products containing hazardous substances, or refinement of non-compatible metals, pre-processing is needed.

Table 4: summarizing conclusions of literature research

Design requirements

These conclusions can be extended to the research into the design of recyclable 3D printed electronics. The main concerns that should be addressed to improve recyclability are the following:

- Embedded components should be accessible for removal.
- Metallurgical incompatible metals should be kept separated in the product, or separation of the incompatible materials should be enabled by design.
- Fine shredding is needed to liberate dissimilar materials and to be able to separate metals from non-metals in the sorting stage. Release of bonds between metals and substrate should be enabled to improve release of dissimilar materials before the sorting stage.
- To allow for the efficient hydrometallurgical refining, circuitry should be made accessible in the recycling process.



figure 9: examples of samples of 3D printed electronics as used in the practical experiments in this thesis.

VISION

From literature studies and preliminary field studies it can be concluded that, with the production technique of 3D printing of electronics still in development, enabling the recycling of the valuable metals and components in the products should be the approach to fit this novel manufacturing method in a circular economy.

While the technique develops further, designers should be supported in the design of recyclable 3D printed electronics. This thesis aims to deliver this support in the form of design guidelines. The guidelines will steer designers towards practices that will improve the access to the components and circuit and increase the liberation of the dissimilar materials in a recycling process. The ultimate goal of enhancement of the design of 3D printed electronics for recycling is to improve the efficiency of the recycling process and preserve the utmost value embedded in the created products.

Establishing the guidelines will be approached in twofold: new methods to improve the liberation of metals from the substrate will be evaluated and iterative experiments will be performed to improve the design of 3D printed objects to fit the conventional and newly found recycling methods.

Practical limitations and opportunities

In the faculty of Industrial Design Engineering of the TU Delft research into 3D printed electronics is conducted (Song et al, 2017; Boekraad, 2017; Maas, 2017). Samples and prototypes for these studies are manufactured with a Voxel8 multi material printer. This 3D printer combines fused deposition modelling (FDM) of PLA substrate with direct write (DIW) printing of a liquid silver paste that can form an electronic circuit when cured (Voxel8 printers, 2017).

In the practical experiments conducted for this thesis that require circuitry, samples will be used that are produced with the Voxel8 printer. These samples are obtained as result from simultaneously performed graduation research (Maas,2017) and come in various shapes, figure 9 shows a few examples of these samples. Shared characteristics for these samples are the use of PLA as substrate and exposed circuitry made from silver.

3D PRINT DESIGN FOR LIBERATION

Design for Liberation is a term used to describe the design of products incorporating measures to enable the liberation of components in the recycling process (Van Schaik, 2013), usually the release of parts of dissimilar materials in a shredder. In the Design for Recycling guidelines (appendix III) several guidelines can be triggers for improving of the liberation of parts in a shredder. However, these instructions are developed for conventional production methods, while the production technique of 3D printed electronics complicates liberation of materials at the end of life, as embedded parts and materials are locked in between fused layers of substrate. The production technique also enables designed weak points in the structure, those weak points will not influence the daily use of the product, but facilitate solutions to improve liberation at end of life. Moreover, the printed outer shell printed around all the integrated parts can also hide design for liberation measures from the user during the regular use of the product before recycling.

Materials & method

In this part of the research constructions were devised to guide the manner in which 3D printed products fracture in a shredder by varying the strength of the local structure of an object. The envisioned constructions were incorporated in the design of simple, small (<10 cm³), objects, which were printed and tested with a bench vice and a modified granulator. Eventually, methods that proved successful were combined to test how breaks can be steered in a way to liberate specific parts of an object.

The tested objects were manufactured through Fused Deposition Modeling from PLA and did not contain embedded electronics. Discoveries based on observations made in these experiments, together with guidelines and characteristics of the current practice of 3D printed electronics, are integrated to draw up guidelines for the design of 3D printed electronics for improved liberation of materials in a recycling process.

Bench vice testing

Samples were first subjected to a test in a bench vice (see figure 10). In a bench vice a sample can be placed so that the leverage points of the applied forces is controlled and the forces will be concentrated in a specific part of the structure, to see if the structure behaves as expected in this specific condition. If this test gave a satisfying result, the same sample was printed multiple times and tested in a modified granulator.

Shredding

Due to the unavailability of a shredder on industrial scale for the experiments, a modified granulator was used. A Zerma GSL 250 granulator (Zerma, 2018), commonly used to grind thermoplastic scrap, was adapted to simulate a shredder by removing the sieve. Without the sieve the granulator consists of nine staggered blades on a rotor that allow chunks with a diameter up to 30 mm to pass through. Figure 11 shows the granulator and its inside.

The magnitudes and leverage points of the forces on the objects in the shredder depend on how the objects fall between the rotating blades. In practice this means that the incorporated measures make the breaking predictable, but not guaranteed. To account for the unpredictability of an object's orientation in the shredder, each model was printed and shredded at least three times.



Figure 10: sample in bench vice

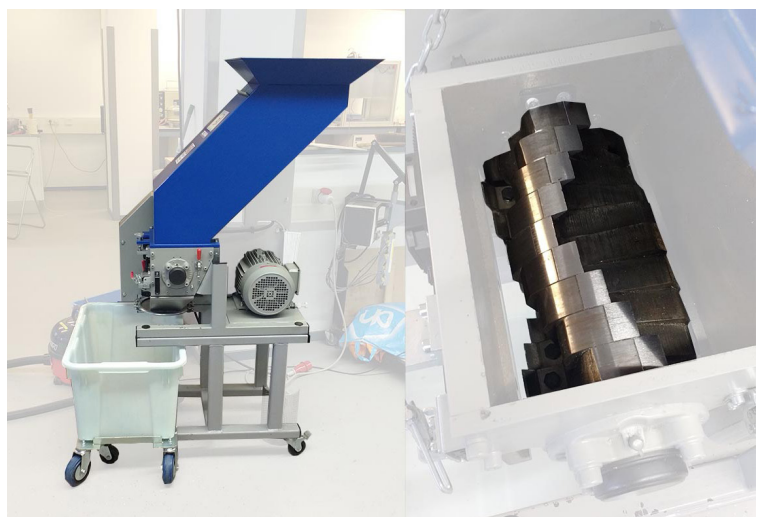
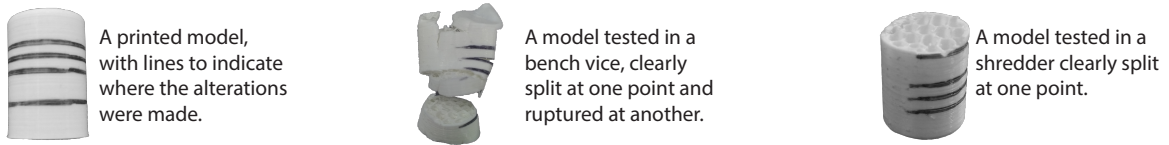


Figure 11: modified granulator and staggered blades

Assessment

Samples were ranked on four scales: visibility, strength, release, and simplicity. When samples passed the first test with the bench vice and were shredded, they were scored on their success rate in the shredder too.



<i>change fill layers</i>		visibility	strength	release	simplicity	shredded	shred result
triangle to grid x3	round tube	2	5	2	3	yes	0/3
triangle to concentric x3 ^	round tube	3	5	5	3	yes	2/3

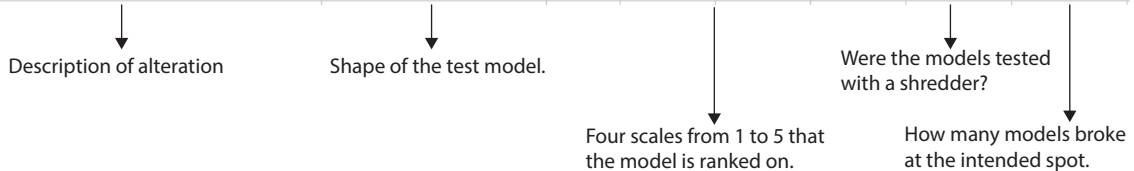


Figure 12: examples of results of samples and ranking scale.

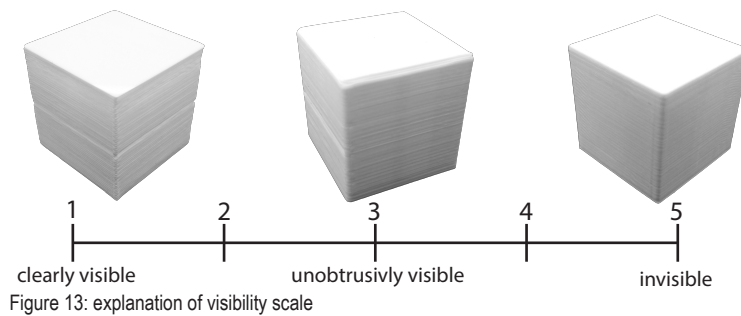


Figure 13: explanation of visibility scale

Visibility

The visibility scale (figure 13) is used to indicate how good the local adjustments were visible regarding the external shape of the model. The visibility was only an issue for objects that had variations in the printer settings over several layers in the z-direction to influence layer adhesion.

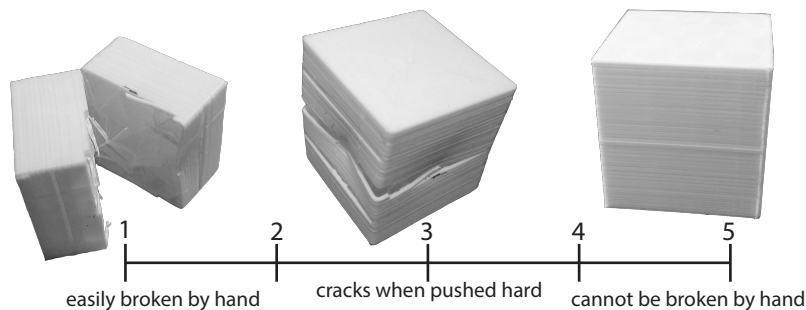


Figure 14: explanation of strength scale

Strength

The functions of 3D printed products and parts should not be influenced by the adjustments made to improve recyclability. Nor should these adjustments lead to a shortened lifespan of the part or product. Therefore the samples were ranked on strength (figure 14), this was not scientifically tested, but rather the author trying to break the objects manually: exercising torsion, bending, and compression stresses on the objects by hand as can be seen in the illustrations in figure 17.

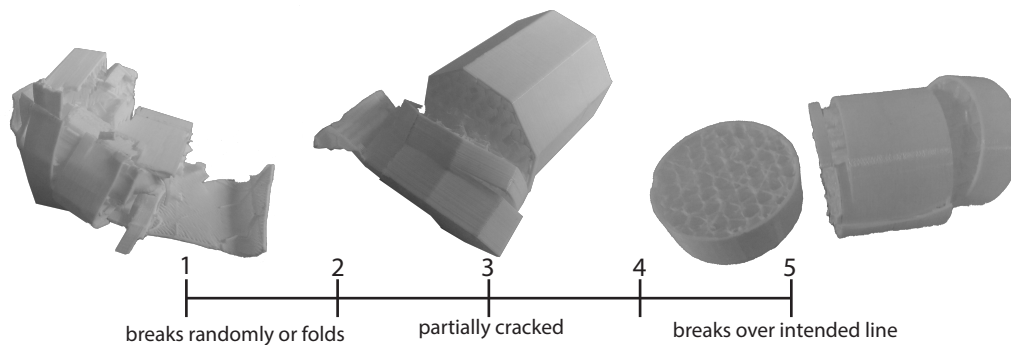


Figure 15: explanation of release scale

Release

Release (figure 15) describes the extent to which the structure breaks in the expected way when tested in a bench vice. In contrast to the aforementioned strength this scale describes whether the object breaks as it is intended to break (over a fracture line for instance) when a controlled force is applied in a bench vice. The strength scale just indicates if the object breaks (when it is not supposed to break) due to manually applied forces.

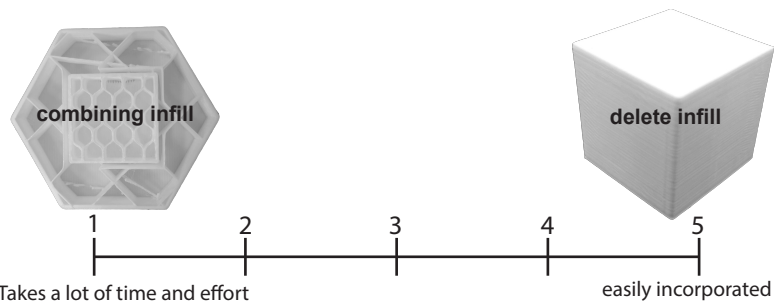
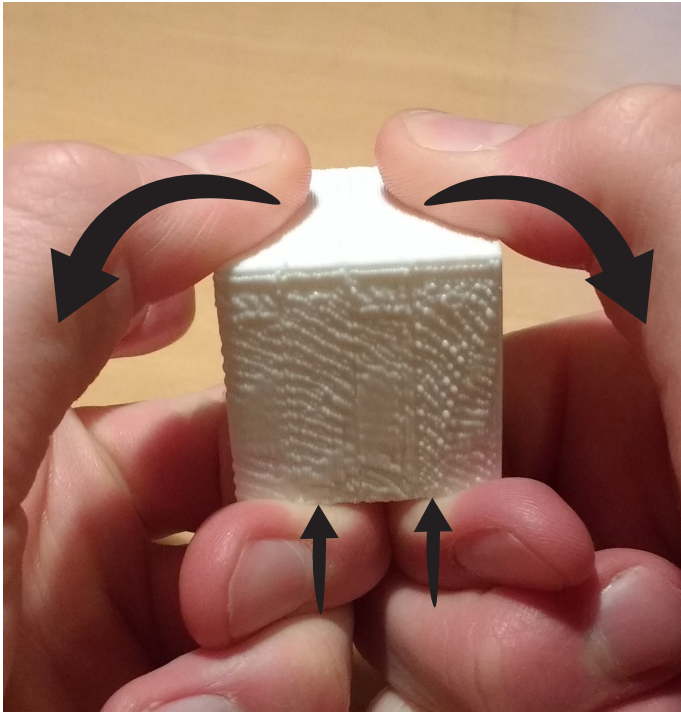


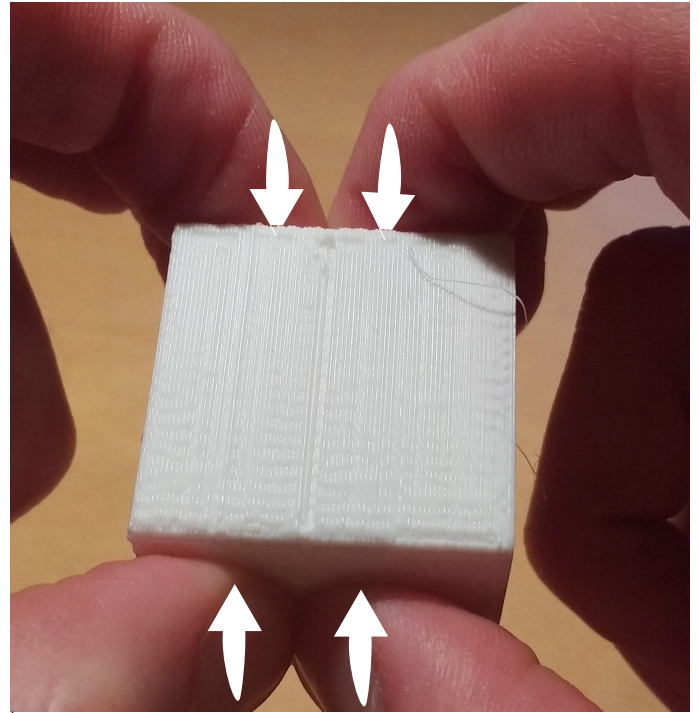
Figure 16: explanation of simplicity scale

Simplicity

Simplicity (figure 16) accounts for the ease with which the construction can be made and incorporated in an object. The ideal solution would take the least effort to implement as it shortens the timespan between iterations in a design process. Due to a lack of options in the software used to prepare 3D prints, most tested objects required manual adjustments in the G-code of the printed objects. G-codes are the lines of code that are sent to a 3D printer to directly command the actions of the printer. For the preparation of the samples for this thesis that meant adjusting thousands of lines of code, however, with the further development of 3D printing as a manufacturing technique, it is expected that more advanced software will facilitate easier incorporation of the local adjustments in printed objects.



a



b



c

Figures 17: illustrations of manual strength tests:

- a bending
- b compression
- c torsion.

Samples

Ideas to selectively create weaknesses in 3D printed parts were derived from knowledge on how common faults occur in a 3D print process. This knowledge was found on internet fora and blogs (Jennings, 2017; Simplify3D, 2018; Brockotter, 2018) where 3D print techniques, tips and tricks are discussed by so called makers, 3D printing enthusiasts with both professional and amateur interests in the subject.

Essentially, all weaknesses in the x or y direction (see figure 18) of the tested prints in these experiments rely on the absence of material or the deposition of less material relative to the surrounding structures to create smaller contact areas and, consequently, concentrating shear stresses at these points. For weaknesses in the z-direction the same approach can be used, as well as decreasing the adhesion between subsequent printed layers by varying in thicknesses of the extruded lines of filament, or by varying in extrusion pattern to decrease the contact area between the layers, effectively increasing shear stresses at these points too.

Using those practices in the experiments, samples were made which were altered in extrusion heights for a small number of layers to either double, triple, or half in height, e.g. two layers were extruded with a height of 0,1 mm while the rest was extruded at 0,2 mm. In other samples, patterns of the infill were altered to change from patterns that are known as strong in the maker community to weaker infill patterns, e.g. three layers (0,6 mm total) change from “triangle” to “concentric” infill pattern. Examples of the infill patterns are shown in figure 19.

In other samples the infill pattern, the inner body of the printed part, was not printed for one, two, or three layers (0,6 mm maximum). The last method to selectively trigger fracture in the z-direction was to reduce wall thickness in the targeted layers by 33%, 50%, and 66%.

To test the guided fracture in the x- and y-directions, small cuts were created on the inside of the walls of the samples, varying in angle, depth, and width. For instance, a 0.6 mm deep cut in a 1.2 mm wide wall with an angle of 45 degrees, as shown in figure 21. Other samples were created with voids over a cross section of the object, varying in shape of the voids and either with or without inner walls (see figure 20).

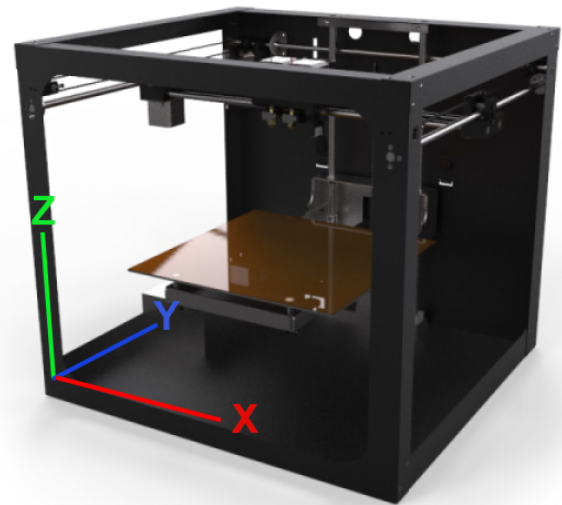


Figure 18: xyz-directions in a 3D printer

To test averting breaks, samples were made featuring double walls with space in between, varying in wall thickness and width of the spacing. Another tested method was the incorporation of infill patterns that are known as strong patterns in a bigger shape filled with weaker infill patterns, for example: a honeycomb filled cube in a grid filled hexagonal tube, as show on the right in figure 22.

As a final step, constructions that proved successful in previous experiments were combined in larger shapes to liberate specific embedded parts. These combinations were made in an iterative way: proven methods were implemented and changed according to the success of the previous tested combination.



Figure 19: different infill patterns, from left to right: honeycomb, wiggly line, concentric, grid, triangular.



Figure 20: three different cross sectional cuts, from left to right: 1mm diagonal with hollow corners, 1 mm cross sectional with walls, 2 mm cross sectional without walls.



Figure 21: cuts in walls schematic slicer preview and photo's: left only in the bottom, right in the bottom and walls.

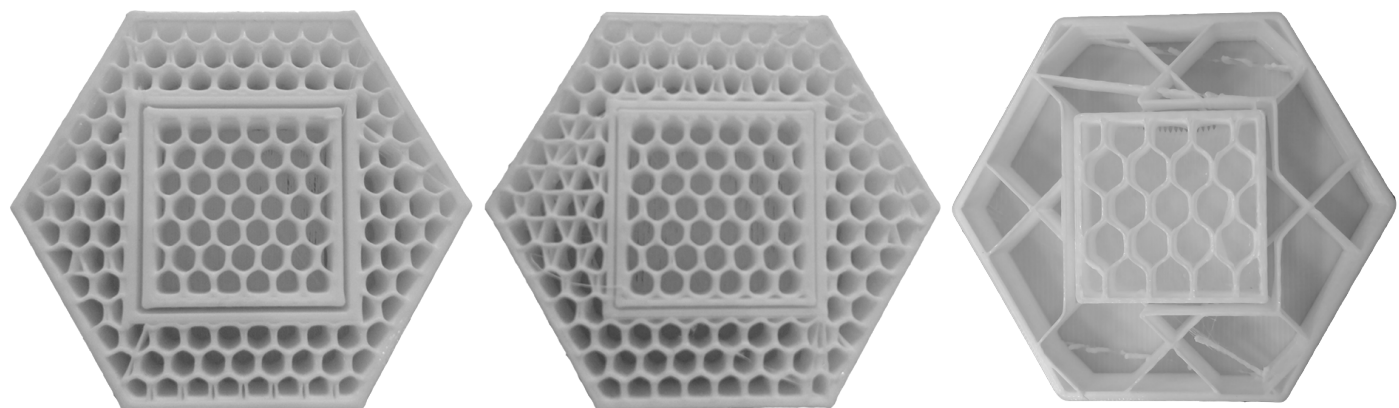


Figure 22: averting breaks; 0.6 mm double walls with 0.7mm space, 0.4 mm double walls with 0.4mm space, combined infill of 15% honeycomb cubel in 5% grid hexagon.

Results

In this section the results from the experiments with the described samples in both the bench vice and the shredder are shown per category. Tables show the results of each tested sample and pictures of results are shown as examples with a description of how the alterations lead to the observed results. A summary of these results can be found on page 30.

Layer Heights

Variations in layer height cause variations in thickness of extruded filament. When the layer height is halved for a number of layers, the contact areas between the consecutive lines of filament is decreased, resulting in concentrations of shear stress in those areas. The illustration in figure 23 shows the decrease in contact area between subsequent layers in a cross section.

Figure 24 shows the result of a sample with double layer height (0.1 to 0.2 mm) pressed in a bench vice. The sample did not split over the intended line.

In figure 25 the result of a sample with four layers of half the normal layer height (0.2 to 0.1) is shown after being pressed in a bench vice. The sample has clearly cracked in the middle, where the smaller layer heights were incorporated.

Figures 26 and 27 show the result of halved layer heights in shredded samples. The sample in figure 26 had four layers of 0,15 mm high incorporated in a cube with layers of 0,3 mm and is clearly split in two halves. The sample in figure 27 shows two parts of a cube with 0.2 mm

layer height and some intermediate layers of 0,1 mm in between.

Table 5 shows all the results of the samples with variations in layer height. It can be observed that the samples with halved layer height gave the best results in terms of release in both the bench vice and shredder.

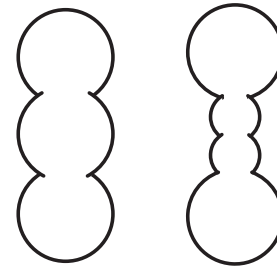


Figure 23: illustration of cross section of fused filament lines. Normal (L) and with two layers of halved layer height (R).

layer adhesion (z-direction)	shape	visibility	strength	release	simplicity	shredded	shred result
<i>double height</i>							
0.1 to 0.2 x1	cube	5	5	1	5	no	
0.15 to 0.3 x1	cube	5	5	2	5	yes	0/3
0.2 to 0.4 x1	cube	4	4	3	5	no	
0.3 to 0.6 x1	cube	2	3	3	5	no	
<i>triple height</i>							
0.1 to 0.3 x1	cube	3	4	2	5	no	
0.2 to 0.6 x1	cube	3	5	2	5	no	
<i>half height</i>							
0.2 to 0.1 x1	cube	5	5	2	5	yes	0/3
0.2 to 0.1 x2	cube	5	5	2	5	yes	0/4
0.2 to 0.1 x4	cube	4	5	3	4	yes	2/4
0.2 to 0.1 x8	cube	3	5	4	4	yes	2/3
0.3 to 0.15 x2	cube	5	3	1	5	yes	0/3
0.3 to 0.15 x4	cube	3	2	3	4	yes	1/3
0.4 to 0.2 x1	cube	5	1	2	5	no	

Table 5: results of samples with variations in layer height.

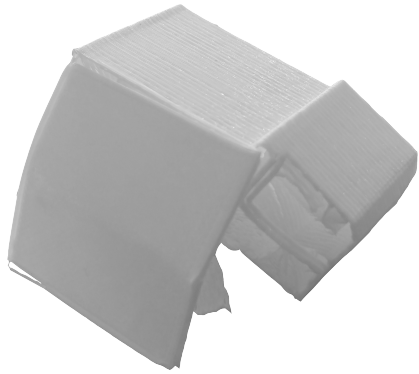


Figure 24



Figure 25

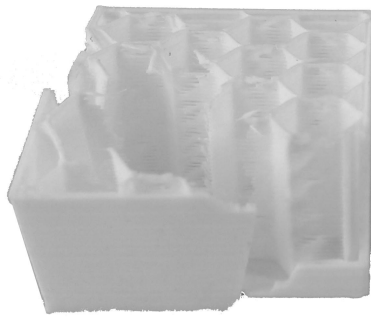


Figure 26

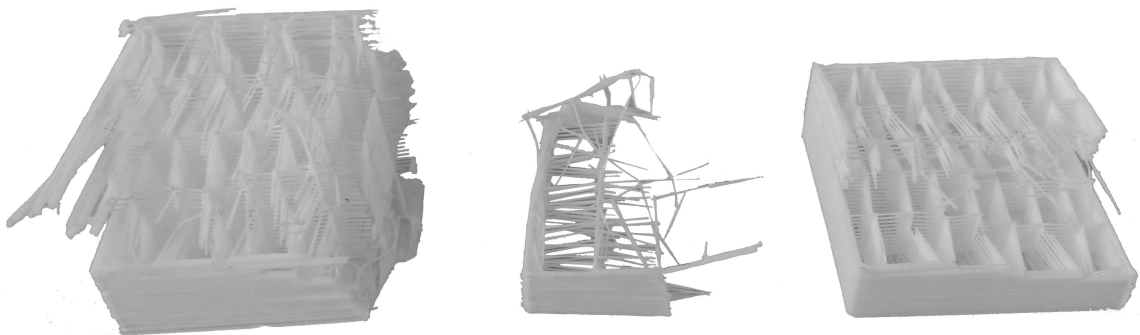


Figure 27

Figures on this page: results of tested samples with variations in layer height: (24). Double layer height for one layer tested with a bench vice. (25) Half layer height for four layers tested with a bench vice. (26) Half layer height for four layers tested in a shredder. (27) Half layer height for eight layers tested in a shredder.

Removing infill layers

Removed infill layers will create samples that are only held together by the outside shell for a small height (ranging between 0,15 and 0,6 mm in these tests). Depending on the orientation of the sample, that will cause concentration of shear stresses on the outer walls in these layers, in theory breaking the sample in a plane over these layers. In the tests with the bench vice, partial fracturing over the intended line was observed before buckling of the sample, as can be seen in the middle of the sample in figure 28. However, these initial results did not persist in consistent satisfying results in tests with the shredder.

Decreasing shell thickness

A decreased shell (outer wall) thickness leads to stress concentrations in the layers with the thinnest shell, as the cross sectional area in the xy-plane is decreased. The results, which can be found in table 6, show that a 50% decrease in shell thickness amounts to a significant release in the tests with the bench vice. Figure 29 shows the result of the bench vice test with a sample with 33% decreased shell thickness; it did not break over the intended line.

Changing infill

By changing the infill pattern for a small number of layers, misalignment between these adjusted layers and the layers above and below it is created. Misalignment causes decreased contact area between subsequent layers, resulting in stress concentrations in the remaining contact areas. In contrast with removed infill layers, the varying infill pattern maintains the stiffness in the xy-plane, preventing the sample from buckling and creating fracture in the z direction. Figure 30 clearly shows a straight cut in a sample tested with a bench vice, where figure 31 shows the same result for a sample tested with a shredder. Both samples had a three layer variation of grid pattern in a sample with honeycomb pattern.

Combined measures for fracture in y-direction

Figures 32 and 33, respectively, show the results of a bench vice test and shredder test with a sample that has a combination of decreased layer height (0.2 to 0.1 mm), variation in infill pattern (honeycomb to concentric), and decreased shell thickness (50%) for six layers. Clear horizontal cuts over the intended lines can be observed. Table 6 shows the results for all the mentioned experiments, and shows successful results were obtained in three out of four combinations of incorporated measures.

<i>remove fill layer</i>	shape	visibility	strength	release	simplicity	shredded	shred result
0.15 -1	round tube	5	5	1	5	no	
0.2 -2	round tube	5	5	3	5	no	
0.2 -3	round tube	5	5	3	5	yes	1/3
0.2 x2: -1,1,-1	round tube	5	5	1	5	no	
0.2 x3: -1,1,-1,1,-1	round tube	5	4	3	5	yes	0/3
<i>change fill layers</i>							
triangle to grid x3	round tube	2	5	2	3	yes	0/3
triangle to concentric x3 ^	round tube	3	5	5	3	yes	2/3
honeycomb to grid x3	round tube	5	5	4	3	yes	3/5
honeycomb to grid x4	round tube	5	5	5	3	yes	2/5
honeycomb to concentric x3 ^	round tube	5	5	4	3	yes	3/5
grid to line x3	round tube	3	5	2	3	yes	0/3
grid to concentric x3	round tube	5	5	4	3	yes	2/3
<i>shell lines</i>							
3 to 2 *^	cube	5	5	2	4	no	
3 to 1 *^	cube	4	3	4	4	no	
2 to 1 *^	cube	4	5	3	4	no	
<i>combined</i>							
L0.2to0.1, honeyc to grid, S2to1 x6	octagonal tube	3	5	5	3	yes	2/3
L0.2to0.1, honeyc to conc, S2to1 x6	octagonal tube	3	5	5	3	yes	3/3
L0.2to0.1, grid to conc, S3to1 x3 ^	octagonal tube	4	5	-	3	only	0/3
L0.2to0.1, grid to conc, S3to1 x6 ^	octagonal tube	3	5	-	3	only	2/3

Table 6: results of samples with variations in layer height.



Figure 28

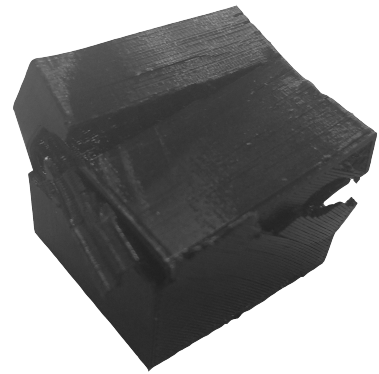


Figure 29

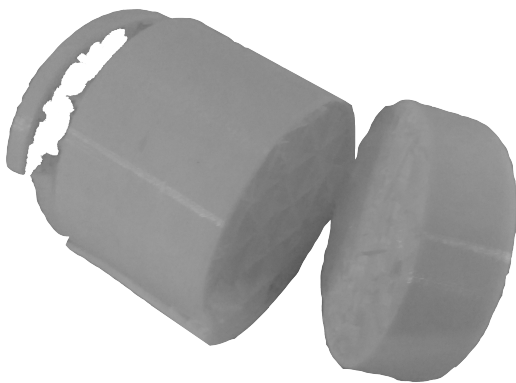


Figure 30



Figure 31

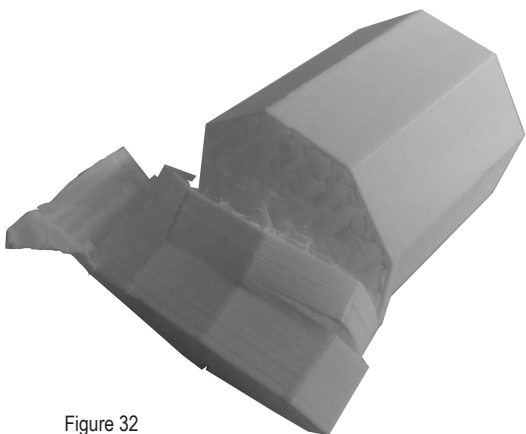


Figure 32



Figure 33

Figures on this page: results of tested samples with variations in layer height: (28). Three removed infill layers tested with a bench vice. (29) 33% decreased shell thickness tested with a bench vice. (30) Changed infill pattern for three layers tested in a bench vice. (31) Changed infill pattern for three layers tested in a shredder. (32) Sample with a combination of decreased layer height, changed infill pattern, and decreased shell thickness tested in bench vice. (33) Sample with a combination of decreased layer height, changed infill pattern, and decreased shell thickness tested in a shredder.

Fracture lines in walls

The fracture lines in walls cause the same effects as decreasing the shell thickness for a number of layers, but it can be applied in more directions than just in the xy-plane. The cross sectional area of the wall is locally decreased, creating stress concentrations. The fracture lines that have angled cuts (see figure 34) create the stress concentrations in the point of the cut, creating more predictable fractures.

Figure 36 shows the result of shredded sample with a 50% cut under a 45° angle in the wall of the object. It is broken and opened, but still partially attached in one wall. Figure 37 shows remains of samples with similar cuts in two planes, the samples are broken in smaller bits but it can be observed that they are broken mainly in the plane with the largest cross sectional area.

Cross sectional cuts

Cross sectional cuts cause the same effects as removing infill layers, but they can be applied in more directions that just in the xy-plane and the cuts do not have to run over the full width of the object. Figure 38 for instance shows a sample with a diagonal cut that is broken in the shredder. Figure 39 shows a part of debris from an octagonal tube with eight intersecting crosssectional cuts

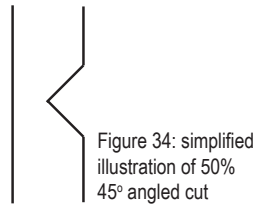


Figure 34: simplified illustration of 50% 45° angled cut

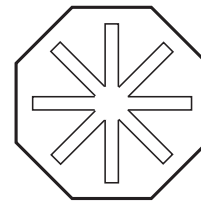


Figure 35: cross section of octagonal tube with 8 cuts

(as illustrated in figure 35), from which can be observed that the object has split in one straight plane, but that the walls around the other cuts keep the structure together instead of facilitating breaking in those planes.

Averting breaks

Breaking of an imbedded object can be averted by creating structures around it that will break and absorb the forces in the shredder. It was found that a balance between thickness of a double wall and spacing between this wall and an imbedded object was required to keep the object from breaking and make it releasable from the outer structure after shredding. Figures 40 and 41 show the results of two different shredded samples in which a cube was imbedded in a hexagonal tube.

The results in table 7 further show that varying in infill pattern and density between the outer structure and the inner embedded object does not yield the desired effect.

Vertical fracture lines (x-or y-direction)	shape	visibility	strength	release	simplicity	shredded	shred result
<i>in walls</i>							
30 degree 80% cut inner walls in 1 plane	flat triangle	5	3	5	4	no	
45 degree 50% cut inner walls in 1 plane	flat triangle	5	4	4	4	yes	3/6
45 degree 50% cut inner walls in 2 planes	flat triangle	5	4	4	3	yes	2/6
1mm straight 50% cut inner wall in 2 planes ^	cube	5	5	4	3	yes	1/3
2mm straight 50% cut inner wall in 2 planes ^	cube	4	4	5	2	yes	2/3
<i>cross sectional</i>							
1mm cross sectional cuts with walls.	cube	5	5	4	5	yes	2/4
2mm cross sectional cuts without walls ^	cube	5	4	5	2	yes	3/3
2mm cross sectional airgaps with walls.	octagonal tube	5	5	-	4	only	0/3
curved cut (max. 3mm) with walls in 1 plane	octagonal tube	5	4	-	5	only	2/4
1mm diagonal cut + hollow corners ^	cube	5	5	-	5	only	1/3
8x 2mm cross sectional cuts with walls ^	octagonal tube	5	3	-	5	only	3/3
averting breaks							
<i>double walls</i>							
2x 0.4 mm walls with 0.4 mm space	cube in hexagonal tube	5	5	-	3	only	0/3
2x 0.6 mm walls with 0.4 mm space	cube in hexagonal tube	5	5	-	3	only	1/3
2x 0.6 mm walls with 0.7 mm space	cube in hexagonal tube	5	5	-	3	only	0/3
2x 0.4 mm walls with 0.7 mm space	cube in hexagonal tube	5	5	-	3	only	2/3
<i>infill</i>							
15% honeycomb cube in grid 5%	cube in hexagonal tube	5	5	-	1	only	0/3
15% honeycomb cube in concentric 10% ^	cube in hexagonal tube	5	5	-	1	only	0/3
15% triangular cube in concentric 10% ^	cube in hexagonal tube	5	5	-	1	only	0/3

Table 7: results of samples with alterations to guide fracture in the x- or y-direction and measures to avert breaks



Figure 36

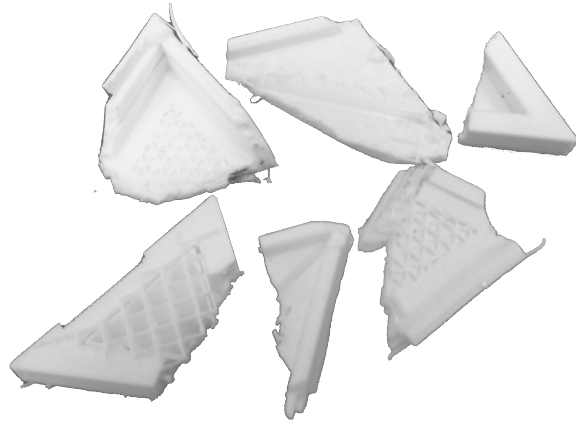


Figure 37



Figure 38

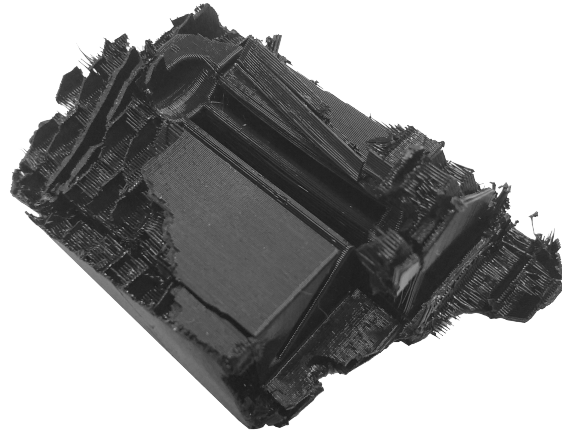


Figure 39



Figure 40

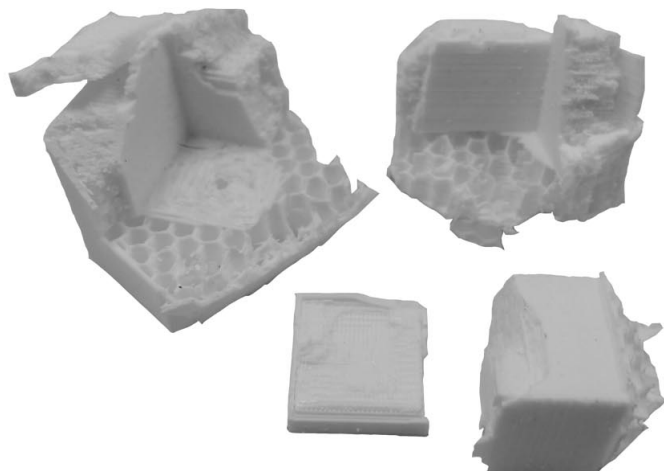


Figure 41

Figures on this page: results of tested samples with various alterations (36) & (37) shredded samples with 50% 45° cut in outer walls. (38) shredded sample with diagonal cut. (39) shredded octagonal sample with eight cross sectional cuts. (40) & (41) shredded samples to test averting fracture around embedded cubes.

Combining measures to release embedded shapes

When the aforementioned alterations to steer fracture in xy-planes were combined with the measures to avert breaking of an imbedded object, the results show that selective destructive liberation of parts is possible, as can be seen in the liberation of the cube in figure 42 from a larger rectangle.

With the incorporation of other measures to create fracture lines in the x- and y-direction, more complex shapes were successfully liberated. Figure 43 shows debris of a similar rectangle with two cubes connected with a rod (seen at the bottom of the image). Both the cubes and the rod are liberated, although not fully intact. In the rest of the debris the walls of the vertical fracture lines can be seen and thin layers of substrate that are broken off in the z-direction due to alterations in layer height.

Figure 44 shows a sample in the shape of a watch from which a pentagon shape with small extending tubes was liberated. This result was obtained by incorporating double walls around the embedded object and creating bad layer adhesion in the layers under and above the

object in the outer watch shape. The results of these experiments can be seen in table 8 and a table with all the results of the experiments with design for liberation measures for 3D printed objects can be found in appendix V.

combining strengths and weaknesses to release inner shapes							
<i>watch shapes</i>	shape	visibility	strength	release	simplicity	shredded	shred result
0.4 mm double walls + 0.4 mm space, 2x half layer height: 0.2 to 0.1 mm above & under.	pentagon in watch shape	5	3	3	3	yes	0/3
0.4 mm double walls + 0.7 mm space, 5x half layer height: 0.2 to 0.1 mm above & under.	pentagon in watch shape	5	3	-	3	only	2/3
<i>rectangles with two cubes</i>							
0.4 mm double walls + 0.7 mm space, 5x half layer height: 0.2 to 0.1 mm above & under.	rectangle with embedded cubes	4	5	-	1	only	1/2
0.4 mm double walls + 0.7 mm space, 5x half layer height: 0.2 to 0.1 mm above & under, 1mm cross sectional cut without walls in 1 plane, removed shell line: 2 to 1, fill:	rectangle with two cubes	4	5	-	1	only	2/4
0.4 mm double walls + 0.7 mm space, 4x half layer height: 0.2 to 0.1 mm above & under, 2mm cross sectional cut with walls in 2 planes, removed shell line: 2 to 1, changed fill honeycomb to grid.	rectangle with two cubes	4	5	-	1	only	2/3
0.4 mm double walls + 0.7 mm space, 4x half layer height: 0.2 to 0.1 mm above, under & middle, 2mm cross sectional cut with walls in 1 plane, removed shell line: 2 to 1, changed fill honeycomb to grid.	rectangle with two cubes	4	5	-	1	only	2/3
remarks:							
nozzle diameter is always 0.4, material is always PLA (jupiter series 123-3D), mostly white 2.85 mm, *= black 1.75mm, infill percentage mostly 10%, ^=15%							
All cubes were 30x30x30mm cubes, the round and octagonal tubes were 40 mm wide by 60mm tall, the triangles were 10 mm high and had even sides of 50 mm.							
In the test with the double walls, the Shred Result number is the amount of (almost) complete cubes that could be liberated in the shredder.							

Table 8: results of samples with alterations to liberate embedded shapes.

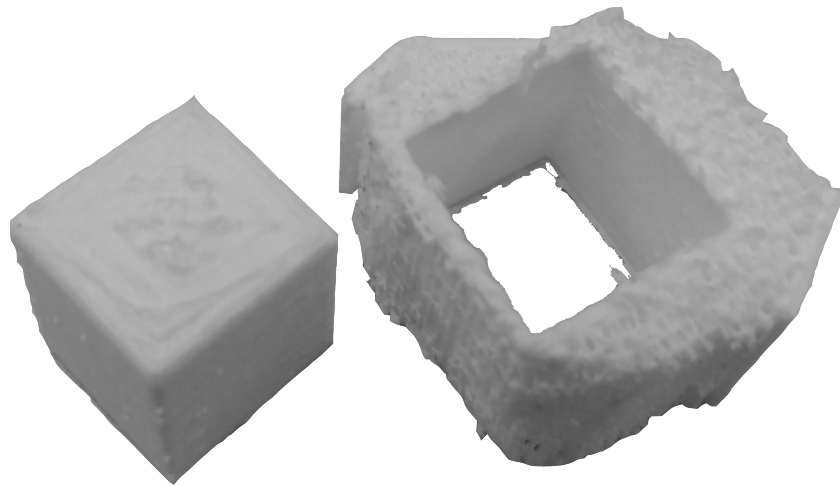


Figure 42

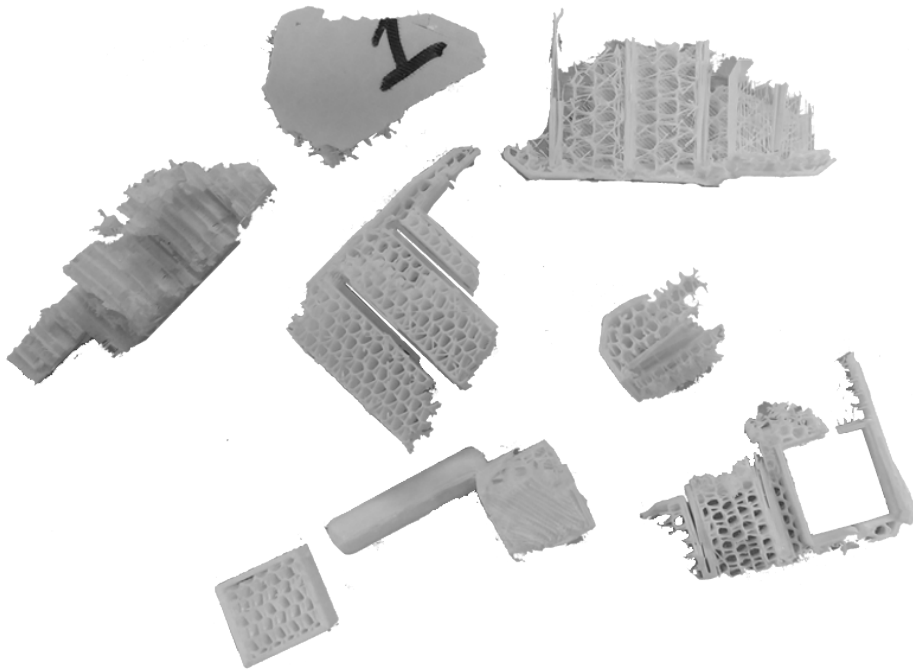


Figure 43



Figure 44

Figures on this page: results of tested samples with combined measures to release embedded shapes. (42) cube successfully liberated from rectangle. (43) two liberated cubes (originally connected by a rod) among debris from a larger rectangle. (44) a 3D printed watch shape (l) and a successful liberated combination of shapes (r) released from the watch.

Summary of results

The results of all the experiments with design interventions to improve liberation of 3D printed objects are summarized in the categorized bullet points below.

Release in z-direction

- Decreasing the layer height by half for multiple consecutive layers will improve the ease of release and the success rate of division in a shredder;
- Removing whole infill patterns in layers will decrease the strength of the printed object while it will not proportionally improve the release;
- Alternating the infill pattern for a number of layers will improve the ease of release and the success rate of division in a shredder;
- Combining a decreased layer height, changed infill pattern, and reduced wall thickness of the outer shell will significantly improve the release along these layers without sacrificing too much of the strength of the object.

Release in x- or y-direction

- Vertical cuts half way through the wall thickness of the outer shell will improve the release along these cuts without sacrificing too much of the strength of the object.
- Creating vertical break lines by implementing airgaps in the infill pattern will improve the ease of release and the success rate of division in a shredder, but having too many, or too wide gaps will decrease the strength of the object. 2 mm gaps seem to be optimal for the size of the tested objects.
- When creating internal voids to guide fracture in the x- or y-direction, having internal walls will increase both strength and stiffness in the object. This results in fracture of the object near the implemented structure, but not necessarily along the intended fracture lines.

Locally strengthening objects

- When using double walls, balance between wall thickness and spacing between the walls is important. Walls which are too thick will not easily break to release the inner structure, spacing which is too small will not release the inner structure either.
- Locally alternating infill patterns will not increase strength sufficiently enough to deflect fracture of the structure in a shredder.

Combined implementation for the release of inner structures

- In combination, the interventions are more effective than applying different methods separately, raising the success rate of the shredder tests from 39% to 50%
- If weaknesses are created in three directions, the success rate is highest for the modifications in the z-direction;
- For flat shapes, a combination of weaknesses in the z-direction in combination with strengthening in the x- and z-direction around the object to be released, seems to have a better result than incorporating weaknesses in all three dimensions.





figure 45: residual debris of samples used in this part of the experimental work.

Implications for design of 3D printed electronics

The implications of these findings for the design of recyclable 3D printed electronics depends on the chosen recycling process. For a hydrometallurgical solution, being able to expose all metal elements to the solvent is required. When considering the pyrometallurgical method, concentration of the valuable metals with the least amount of polymer substrate is desired, as noted in the chapter on electronics recycling (page 11).

The results from the experiments show that successful division between consecutive layers can be obtained by combining alterations in layer height and infill pattern, and reduced wall thickness of the outer shell. For the design of printed electronics this means that where possible, (large parts of) the circuit should be printed in the x-y plane. When liberation of the circuit for pyrometallurgical refining is intended, having the circuit in a plane will allow breaking off of parts below and above that part of the product, concentrating the circuit's metals in a smaller "sandwich" of substrate. An illustration of this principle is shown in figure 46b.

When preparing the electronics for hydrometallurgical treatment, having the circuit in a plane will allow splitting the product at the height of the head space above the circuit, and making the circuit accessible to solvent. This principle is illustrated in figure 46c.

The result further show that multiple methods can be used to steer how an object breaks in a shredder and that good results can be obtained by combining weakened structures with stronger, break deflecting structures to liberate specific parts from the rest of the object. These adjustments to avert breaks at certain points require extra space in the object and deposition of additional material to locally strengthen the product.

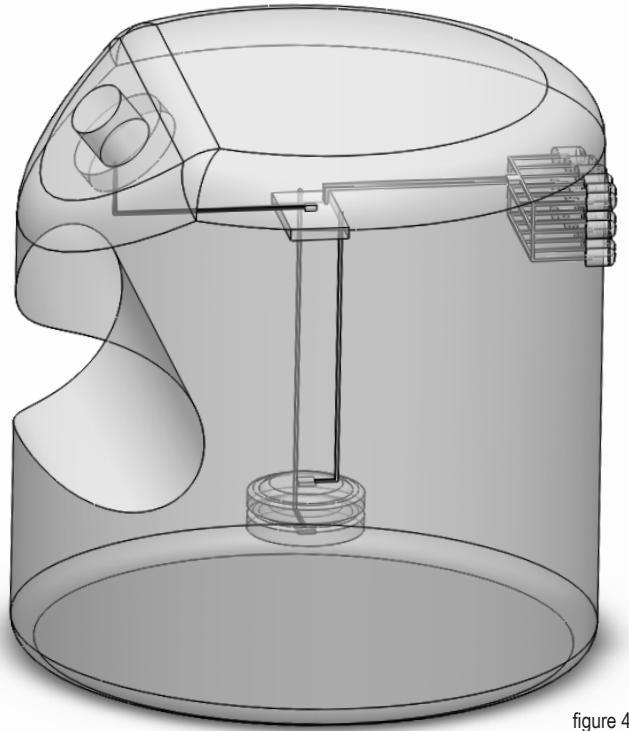


figure 46a

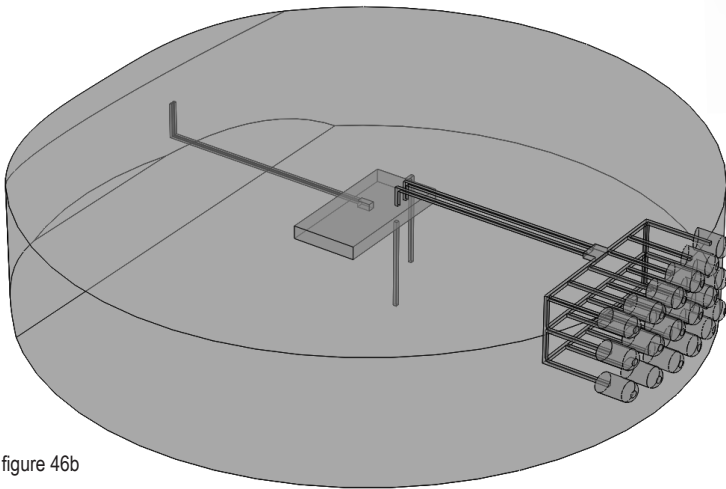


figure 46b

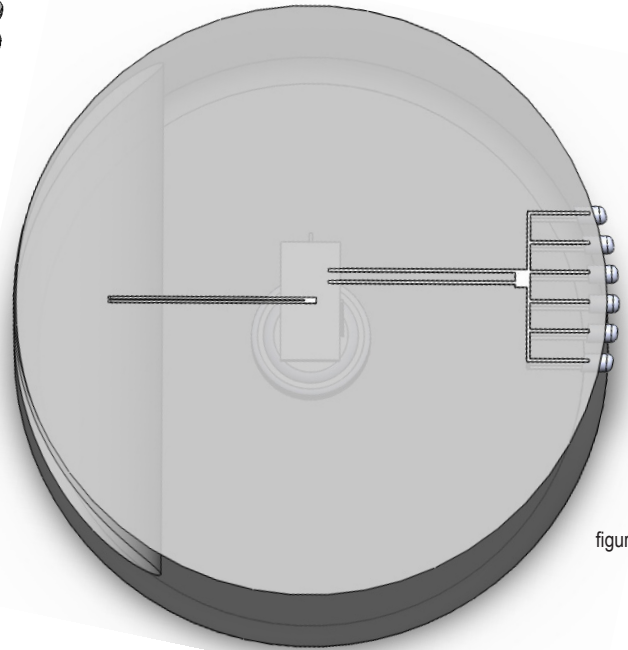


figure 46c

Figures on this page:

46a: Example CAD design of a 3D printed bike light with embedded electronics, consisting of a push button, resistor, controller, batteries, and LED's.

46b: "Sandwich" part of the bike light with most of the electronic components and circuitry concentrated in a smaller part of the substrate. Weaknesses are incorporated in the layers above and below this "sandwich" to break off the redundant parts in a shredder.

46c: Adjusted design of the bike light for hydrometallurgical treatment, with the circuitry made accessible. A large part of the circuitry is deposited in one plane; the number of LED's is lowered to only one row in one plane, and the push button is placed so that the circuit can be deposited in the same plane. The layer above the circuit is weakened to break off in a shredder.

EXPLORATION OF METHODS TO RELEASE SILVER CIRCUITRY FROM PLA SUBSTRATE.

From the review of current recycling processes (page 7) it can be concluded that methods are in place to sort and purify metals that are liberated when electronics are shredded in the process. An experiment in which 3D printed electronics were shredded showed that the silver traces did not release from the bigger substrate granulate, which will cause middlings in the sorting process and impurities in the purification, reducing the overall yield of the recycling process.

To improve the liberation of dissimilar materials in the recycling process, a method is required to detach the silver circuitry from the substrate. This method could either be used as a step prior to shredding, so that the material releases in the shredder, or as a treatment of the shredded product before sorting of materials. The method has to be applicable to treat products in a range of sizes in a cost and time efficient manner on an industrial scale.

Four methods were devised to achieve this goal, all relying on the difference in thermal properties and partially relying on electric properties of the two materials. In this part of the research these methods were tested on their feasibility, observations were used to draw conclusions on promising directions for further research, and the implications on product design were considered for the implementation of these methods. In the conducted experiments for this study release from the silver also means liberation of the material from the product as the used samples had external circuitry, while in a recycling process of 3D printed electronics release of circuitry is a step towards liberation of the metals from the containing product.

Methods

Induction

When an (electronic) conductor is placed in a changing magnetic field a voltage is generated, driving a current through the conductor. When current flows through the silver, resistive heating will cause it to heat up. This could possibly be used if products were to be sent through the middle of a coil with an alternating current, generating a current through the silver circuitry that dissipates enough power to melt the first contact layer between the circuit and substrate and not melt the PLA at depth.

Microwaves

Microwaves are a form of electromagnetic waves with high frequencies. The changing magnetic field can induce a current flow in conductive material (Morgan, 1949). This could possibly be used to induce eddy currents in the embedded circuits of the still closed products and generate a current that dissipates enough power to melt the first contact layer between the silver circuit and substrate and not melt the PLA at depth.

Hot water

The third method to be tested is weakening the substrate-circuit bonding by heating the printed object as a whole in near-boiling water. The used PLA has a glass transition temperature (T_g) of 55-60°C, melting temperature of 210°C, and heat distortion temperature (HDT) of 80-90°C (NatureWorks, 2016).

The T_g is the temperature range at which amorphous material becomes flexible, while the HDT is a measured temperature at which a certain deflection is measured in a standardized test, used as an indication of a temperature above which the material cannot be used for structural applications (Polymer Database, 2015). By immersing the printed object in hot water as a whole, the PLA substrate will become flexible while the silver does not change. This can possibly be used to weaken the bond between the silver and PLA.

Furthermore, the thermal expansion coefficient of PLA is $41 \cdot 10^{-6} \text{ K}^{-1}$ (SD3D, 2017), while silver has a coefficient of $18 \cdot 10^{-6} \text{ K}^{-1}$ (Nave, 1999), indicating that PLA when heated will expand more than the silver, resulting in stresses in the contact layer between the two materials.

Ultrasounds

Following from the hot water experiments another tested method was added using ultrasounds. Ultrasonic cleaners have high frequency transducers on the bottom of a fluid filled tank that create pressure waves in the fluid, that in turn create cavitation bubbles. When these bubbles implode near objects immersed in the fluid, they exert powerful forces on the objects (Ensminger & Bond, 2011). In these experiments the chosen fluid is hot water, to weaken the bond between the circuit and substrate as described before. The shock waves in the water can possibly be used to force the circuit from the substrate.

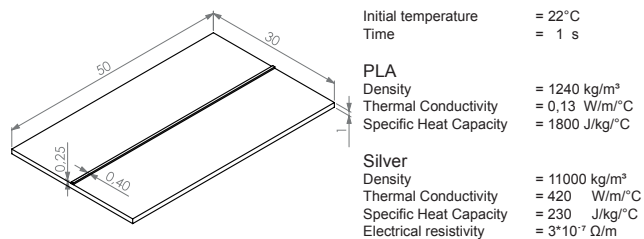


Figure 47: Ansys Workbench heat dissipation settings

Method 1: Induction

The feasibility of the induction method is determined by the required conditions to induce this current in the circuit. First a FEM simulation is conducted in Ansys Workbench (Version 18.2, Ansys Inc, 2017) to find the required resulting current in the circuit for this goal. In the simulation a 50 mm long straight track of silver is modelled with a width of 0,4 mm and height of 0,25 mm on a 1 mm thick PLA substrate layer, as can be seen in figure 47. The single track enables an indication of the magnitude of the current per set distance to be found, so that the result can be validated with tests on physical samples. In the simulation a target temperature of 316°C was chosen as this is the decomposition temperature of PLA (Ohkita & Lee, 2005).

The dimensions of the track and thickness were chosen to match those of the available samples. The samples were obtained from graduation research (Maas, 2017) into 3D printed electronics and manufactured with a Voxel8 multi-material printer. Some of the samples can be seen in figure 48.



Figure 48: examples of used samples, 3D printed PLA and silver manufactured with a Voxel8 multi-material printer. Not to scale.

In Ansoft Maxwell (Ansys Inc, 2015) two other simulations were performed to examine whether the required resulting current can be induced as proposed. In the first simulation a coil is modelled with a 50 mm long straight silver track in its core, as shown in figure 49. Parameters of this coil were chosen to match a small scale installation in ideal conditions.

To explore the full potential of inductive heating, a second simulation was performed with adjusted parameters. The diameter of the coil was decreased from 300 mm to 6 mm and the frequency increased from 57 kHz to 300 kHz, as shown in figure 50. The number of turns on the coil was not increased as the magnetic field strength does not significantly increase with a higher number of turns with these dimensions (Khazaal et al., 2016).



Figure 49: setup of first induction simulation

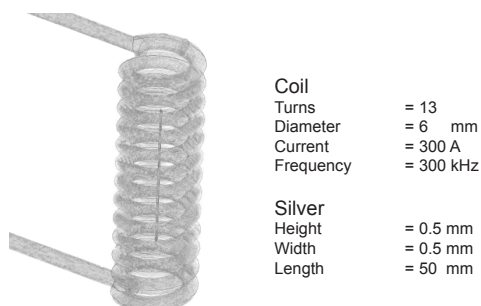


Figure 50: setup of second induction simulation.

Results: Induction

In figure 53 the result of the heat dissipation simulation is shown, it shows that a power of 24 Watt needs to be dissipated in one second in the resistive heating of the track to reach the desired temperature.

This required power leads to a current of 12,6 A, calculated as follows:

$$P = 24 \text{ W} \quad P = I^2 \cdot R$$

$$l = 50 \text{ mm} \quad R = \frac{\rho \cdot l}{A} \quad I = \sqrt{\frac{\rho \cdot l \cdot P \cdot h \cdot b}{\rho \cdot l}}$$

$$h = 0,25 \text{ mm} \quad b = 0,4 \text{ mm} \quad \rho = 3 \cdot 10^{-7} \Omega \cdot \text{m} \quad A = h \cdot b$$

This current was applied to parts of circuit of approximately 50 mm in length on the available samples, some of which are shown in figure 51. The intended result was obtained: the silver tracks detach from the PLA and seem to jump up off the substrate, the circuit is broken and current flow is interrupted. Incrementally the current was lowered to 10 A, showing consistent satisfying results at 11 A.

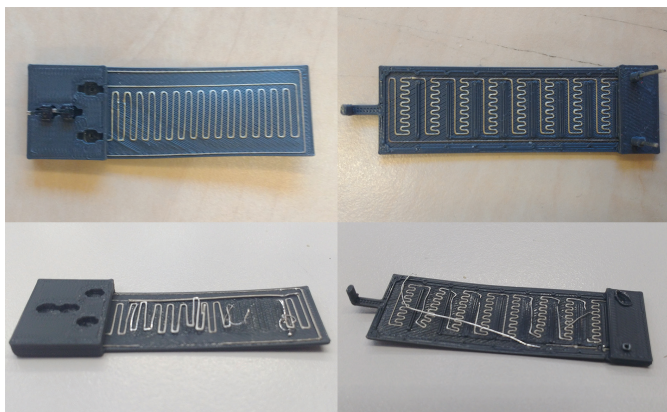


Figure 51: samples before and after high currents (12,6 - 10 A) are applied with contact electrodes.

After applying the current to the samples, the circuit and substrate were analysed with a microscope to determine whether the bond between the silver and PLA had indeed decomposed as expected. The decomposition was confirmed, the pictures and conclusions from this analysis can be found in appendix VI, one of the microscopy images is shown in figure 52.

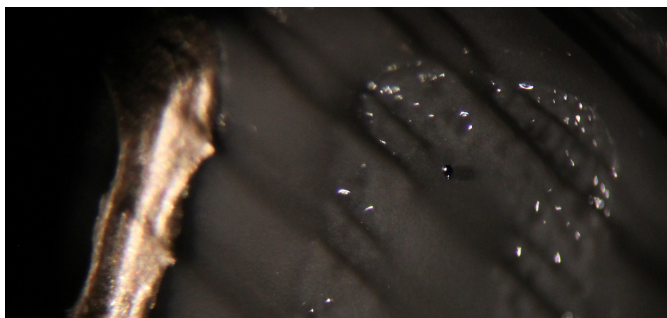


Figure 52: microscopy image of test sample: a silver track still attached to the substrate on the left, an impression of molten substrate where silver was attached on the right.

The second simulation, a FEM analysis of the induction of a single track in a coil with a diameter of 300 mm, gave as result that a current of $6,3 \cdot 10^{-4}$ A was induced in the track in these conditions, as shown in figure 54.

The last simulation, of a single track in a coil with improbable parameters, resulted in an induced current of 0,26 A as shown in figure 55.

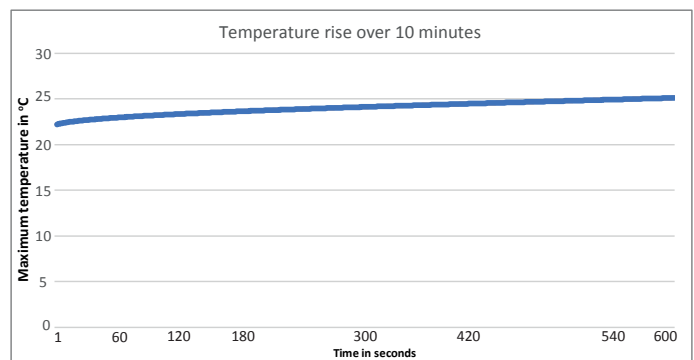
The resulting currents in both simulations are far below the required 11 A needed for the decomposition of the contact layer.

In the experiments with hot water (page 40) the goal is not to reach the decomposition temperature of 316°C but to heat the object to above the glass transition temperature (Tg), between 60°C and 100°C. Another simulation was run in Ansys Workbench to analyse whether the maximum current that could be induced according to the simulation with improbable parameters, could be used to heat the substrate near the circuit to temperatures above the Tg.

Figure 56 shows the result of a simulation in which 0,26 A was applied for 10 minutes; the temperature rises from 22 to 25,1°C. In the image the result of the simulation is shown as heat distribution over the cross section of the model. The current, power, and time of power dissipation are shown on the right.

Graph 1 shows the rise in temperature over these 10 minutes, displaying that a rise to a temperature above the Tg, even in the ideal conditions of the simulation, would be too slow to be viable on any scale.

The conclusion can be drawn that for this goal induction will not be suitable either.



Graph 1: simulated temperature rise in circuit with 0,26 A applied over 10 minutes.

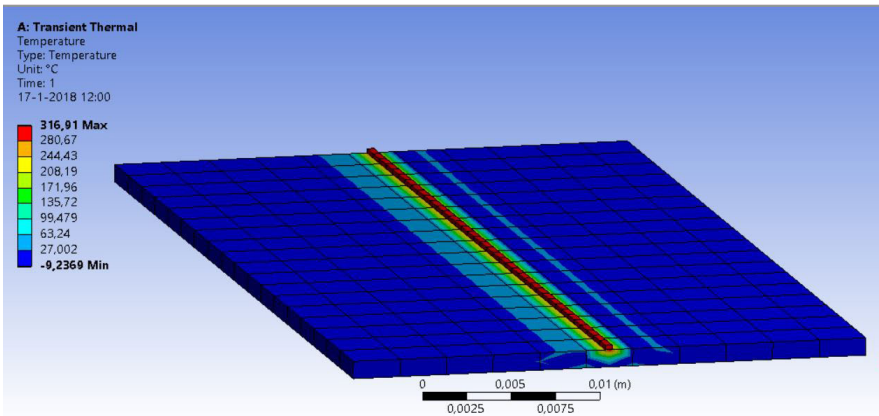


Figure 53: result of the heat dissipation simulation.

Initial temperature = 22°C
 Time = 1 s
 Maximum temperature = 316,91°C
 Dissipated power = 24 W

PLADensity = 1240 kg/m³
 Thermal Conductivity = 0,13 W/m°C
 Specific Heat Capacity = 1800 J/kg/°C

Silver
 Density = 11000 kg/m³
 Thermal Conductivity = 420 W/m/°C
 Specific Heat Capacity = 230 J/kg/°C
 Electrical resistivity = 3*10⁷ Ω/m

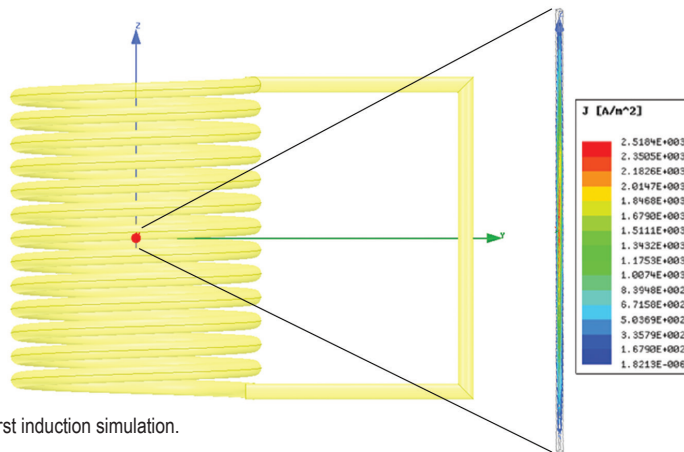


Figure 54: result of the first induction simulation.

Coil
 Turns = 13
 Diameter = 300 mm
 Current = 300 A
 Frequency = 75 kHz

Silver
 Height = 0,5 mm
 Width = 0,5 mm
 Length = 50 mm

Maximum induced current
 $2,52 \cdot 10^3 \cdot 5 \cdot 10^{-4} \cdot 5 \cdot 10^{-4} = 6,3 \cdot 10^{-4}$ A

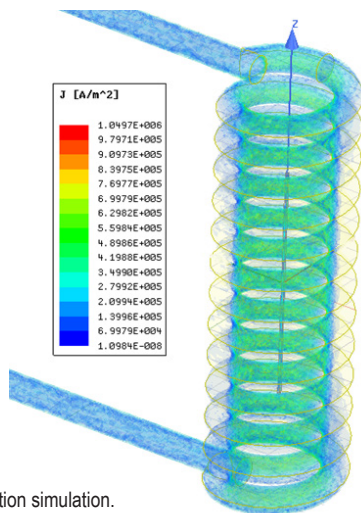


Figure 55: result of the second induction simulation.

Coil
 Turns = 13
 Diameter = 300 mm
 Current = 300 A
 Frequency = 75 kHz

Silver
 Height = 0,5 mm
 Width = 0,5 mm
 Length = 50 mm

Maximum induced current
 $1,05 \cdot 10^6 \cdot 5 \cdot 10^{-4} \cdot 5 \cdot 10^{-4} = 0,26$ A

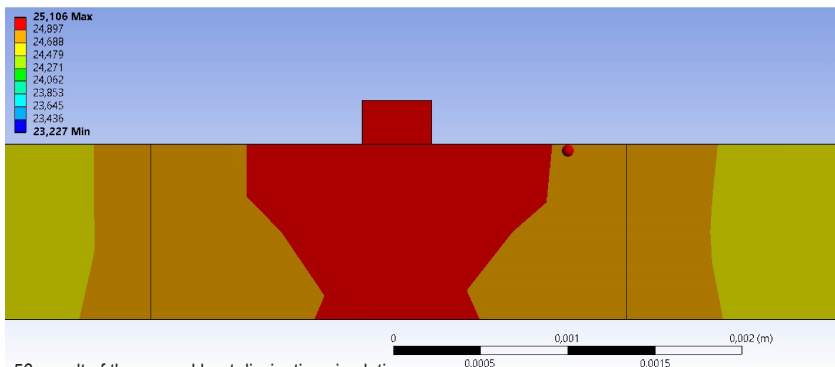


Figure 56: result of the second heat dissipation simulation.

Dissipated power = 0,01 W
 Time = 800 s
 Current = 0,26 A
 Maximum temperature = 25,1°C

Method 2: Microwaves

The experimental feasibility of the use of microwaves for the intended goal was tested with a common microwave oven (a Sharp R-870A, as shown in figure 57), operating at 2,45 GHz providing 900 Watts. For these experiments similar samples were used as mentioned before, obtained from graduation research into 3D printed electronics at the faculty of Industrial Design Engineering at the TU Delft. To achieve consistent results the turntable plate was removed from the microwave oven and the optimal spot in the oven to place the samples was found. This place was found by repeatedly heating a wetted cardboard briefly and registering the dried areas.



figure 57: Microwave oven with optimal spot indicated.

Samples were placed in the same spot for all tests, power and time were varied. Power was changed in percentages of the maximum power output, as allowed by the microwave oven. Time was varied from 20 to 2 seconds per test (as indicated in table 9), starting with long intervals and gradually working to lower timespans in an iterative way, stopping the microwave oven as reactions were observed.

Power (W)	Time (s)		
900	20	10	3
630	15	5	2
450	10	6	2
270	5	2	
90	20	10	3

table 9: variations in power and time in microwave experiments

Results: Microwaves

Table 10 shows the results of the experiments with the microwave oven, figure 58 shows some examples of the results. The microwaved samples were either very locally heated, removing the silver but making it unrecoverable (figure 58a), or melting the PLA along a track, warping the substrate and circuit combination (figure 58b), fusing these together more instead of separating them.

To be able to draw conclusions from the results, a surface graph was made that shows the effects of power and time in these experiments. The size of the affected areas was ranked on a scale from 1 to 5, with 5 being the largest affected area. The vertical axis of the surface graph, shown in graph 2, indicates power, the horizontal axis shows time, and the affected area size is shown in colours.

It can be observed that the highest peaks (the largest affected surfaces) are on the right side of the graph, indicating that a longer exposure time results in further melting and warping of the substrate. The most peaks appear in the upper right corner of the graph, suggesting that increased power too will lead to larger affected areas. It should be noted that a larger sized affected area does not correlate to a higher release rate of silver in these experiments.

During the experiments it was observed that when only a very small area is affected, increasing the exposure time will not result in more reaction. A possible explanation for the behaviour can be found in the non-uniform shape of the cross sections of the track. As can be seen on the microscopy images (see appendix VI), the silver traces do not have a straight smooth surface, but have spikes and dents along their upper surface. The microwaves induce high potential around the sharpest of these edges (Morgan, 1949), creating sparks that cause discharge through the air and break the circuit. When the 3D printer is able to deposit the silver more uniformly, this might improve consistency in the results. Another possible explanation can be sought in the non-uniform distribution of microwaves in the microwave oven. Despite the localisation of the optimal place in the oven to put the samples, the distribution of waves can be of a decisive factor in the results.

The results of these experiments with a microwave oven show that within the limitations of this study, microwaves do not give satisfying results for the intended goals. However, the limitations in this study were set by the use of a consumer grade microwave oven with limited customizability with regards to transmitted power, time of exposure, and distribution of the microwaves over the samples.

Power (W)	Time (s)	Result
900	20	1 spot silver gone, one arm warped.
900	10	1 spot silver gone, one arm warped.
900	3	melted and flexible PLA, not released.
630	15	PLA disintegrated, melted and warped. Silver tangled up.
630	5	melted and flexible PLA, not released.
630	2	1 spot silver gone
450	10	PLA molten and warped, silver partially loose.
450	6	Partially disintegrated, partially warped, PLA and silver tangled.
450	2	melted and flexible PLA, not released.
270	5	Substrate warped, 1 spot silver gone.
270	2	2 spots silver gone, flexible substrate.
90	20	PLA disintegrated, melted and warped. Silver tangled up.
90	10	1 spot silver gone, flexible substrate.
90	3	1 spot silver gone.

Table 10: results of microwave experiments.

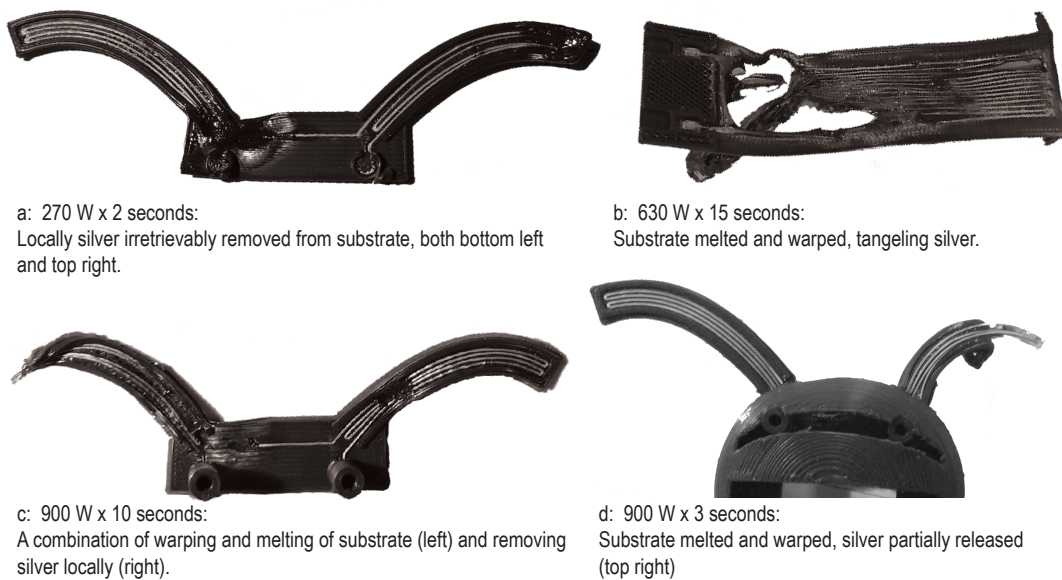
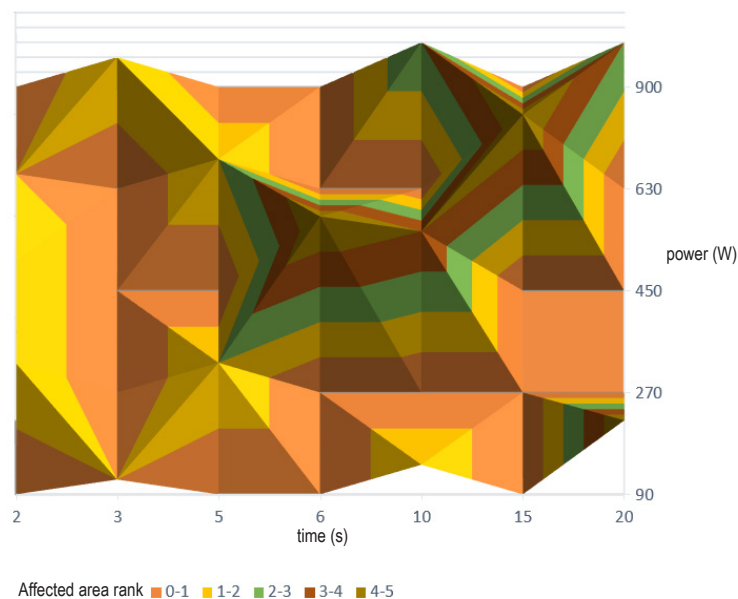


Figure 58: examples of results of microwave experiments.



Graph 2: surface graph of results of microwave experiments. Time is shown on the horizontal axis, power on the vertical axis, the colours indicate the affected area size.

Method 3: Hot water

The experimental feasibility of the method with hot water was tested by submerging samples in near-boiling water. Variations were made in immersion time and in how the sample was handled in and out of the water. A part of the samples was just submerged in the water, others actively budged by shaking them in the water, a share of samples was bent after immersion, some were flushed with hot water from a kettle, and from others the tracks were brushed after submersion.



Figure 59: materials used for experiments.

The experiments were performed by heating (approximately) 200 ml water on an electric stove. The temperature of the water was measured with a conventional thermometer (see figure 59), the temperature varied over the time of the experiments as samples were immersed in the water in sequence. To examine whether the desired effect displays above T_g or HDT, a share of the samples was submerged in water at a temperature above the T_g but below HDT of PLA.

The samples were held in the water with pinchers. For these experiments similar samples were used as mentioned for the other experiments. In total 16 samples were used for these experiments.

Results: Hot Water

Of the four tested methods, heating the objects as a whole in boiling water gave the best results within the limits of these experiments. Figure 60 shows the results of the tests with samples 2, 4, and 8. The results of all performed tests are noted in table 11.

The results show that keeping the samples stationary in hot water does not release the silver from the PLA, but that applying forces that make the circuit move relatively to the substrate will result in release of the silver. Successful methods to create this relative movement are bending of the flexible substrate, shaking the sample in the water, and brushing the surface of the sample lightly once with a finger after immersion. Pouring kettle water (with a varying temperature between 95°C and 90°C) over the surface of the sample to create movement did not lead to the intended result.

The results of these experiments justify further research in this direction. Methods that led to release of the silver in these tests did not yield consistent success rates in terms of released percentages of silver circuitry. No significant conclusions can be drawn regarding the best processing time or temperature based on these results. The results do indicate that release of the silver occurs above the T_g and is not limited to temperatures above the HDT, although it can be observed that the highest percentages of release and the shortest immersion times before release all occurred in the experiments with temperatures above 90°C. This also does not rule out that the release is the effect of stresses in the materials due to the differences in thermal expansion coefficient.

Inconsistent success rates in these experiments might be ascribed to the variety in shape of the used samples, irregularities in the production of the samples due to the immaturity of the novel production technique, or slight variance in the reproduction of procedures during the experiment by the author.

sample	t (s)	T (°C)	action	result	secondary action	result
1	15	95	shaking	80% released		
2	5	90	shaking	warped, not released		
	+5	90	shaking	100% released		
3	5	92	static	warped, not released		
	+5	91	static	warped, bits loose	Brushed	50% released
4	10	91	static	warped, not released		
	+30	91	static	loose, not released	Bent	100% released
5	10	98	static	barely warped		
	+10	95	shaking	50% released		
6	10	93	shaking	30% released	Bent	80% released (total)
7	240	98	static	warped, not released	brushed	80% released
8	120	89	static	warped, not released		
	+60	90	shaking	80% released		
9	30	89	shaking	60% released		
10	20	96	static	-	flushed with kettle water	warped, not released
	+20	96	static	-	flushed with kettle water	warped, not released
11	60	90	static	-	flushed with kettle water	warped, not released
	+60	92	static	-	flushed with kettle water	warped, not released
12	60	91	static	-	flushed with kettle water	warped, not released
	20	91	shaking	30% released	brushed	100% released (total)
13	120	68	shaking	flexible not warped	Bent	60% released
14	60	66	shaking	flexible not warped	Bent	98% released
15	30	69	shaking	70% released		
16	60	68	shaking	20% released		

Table 11: results of hot water experiments.



Figure 60: examples of results of hot water experiments

Method 4: Ultrasounds

As the experiments with hot water yielded promising results but showed that forces need to be applied to make the circuit move relatively to the substrate before it releases, ultrasonic cleaning was suggested to induce this movement. The experimental feasibility of this method was validated with the use of a Branson ultrasonic cleaner model 1510E-DTH (Branson Ultrasonic S.A., 2007), as shown in figure 61. This cleaner has an internal thermostat that can heat the water up to 69°C and induces sonic waves at a fixed frequency of 42 kHz. Water was externally heated in an electric water heater before being used in the cleaner. Four consecutive batches of 3 samples were immersed in the cleaning bath. The samples used are similar to the samples used in the experiments described before. For each batch the time of immersion was increased and the temperature was lowered.



Figure 61: Bransonic model 1510E-DTH.

Results: Ultrasounds

Table 12 shows the results of the experiments per sample. Examples of the results can be seen in figure 62, where samples are shown before and after treatment in the ultrasonic cleaner.

The results indicate that silver is released from the samples in the ultrasonic cleaner. Although no consistent results were obtained per batch, the results show that higher temperatures increase the rate of release.

The shallow and open tank of the ultrasonic cleaner lead to a decrease in temperature during the experiments. The noted temperatures are the temperatures as indicated by the thermostat of the apparatus at the start of each batch.

The highest released percentage of silver in these experiments was 50%. Drawbacks of the machine used were the fixed frequency of induced sonic waves at 42 kHz and the inability to maintain a high fluid temperature. A suggestion for future research (page 48) is a repetition of these experiments with higher temperatures and lower frequencies, as this might improve the released percentage of silver.

It was not recorded at what time the circuit released from the substrate and whether this was time dependent. The results do not show an increase in release percentage over time, but this might be ascribed to the decreased fluid temperature over time.

sample	T (°C)	t (s)	% released
1	82	360	20
2	82	360	50
3	82	360	15
4	72	390	5
5	72	390	5
6	72	390	50
7	67	420	0
8	67	420	2
9	67	420	5
10	61	480	0
11	61	480	30
12	61	480	0

table 12: results of the ultrasound experiments.

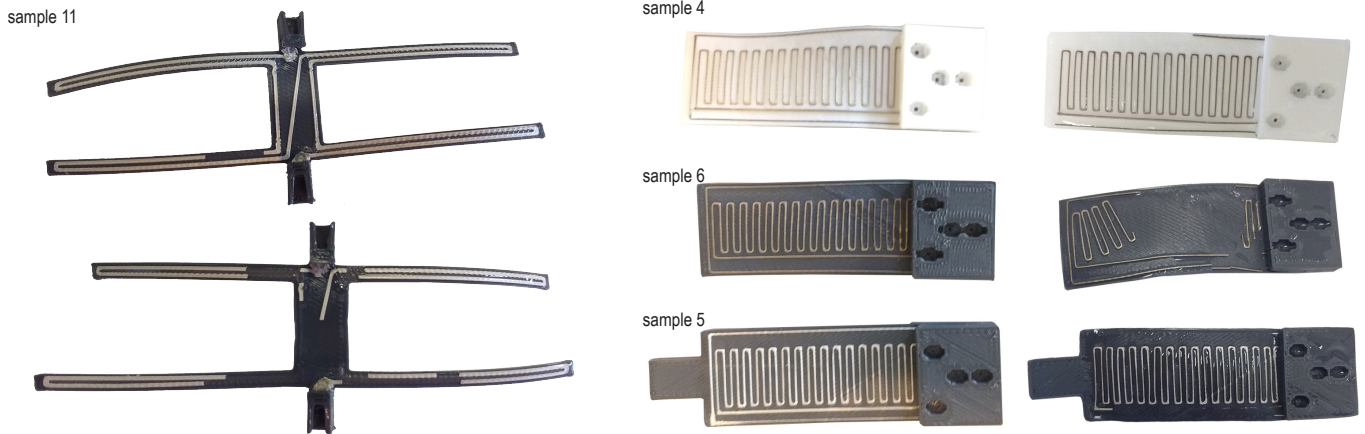


Figure 62: Samples before and after treatment in the ultrasonic cleaner. Samples shown: 11, 4, 5, and 6.

Discussion of methods and results

In this explorative research four methods were investigated on their suitability to release silver circuitry from PLA substrate. The goal of the release of the silver is to improve the liberation of metals from 3D printed electronics in a recycling process. This explorative research raises a lot of questions too, which might be answered by follow-up researches. These questions are discussed on page 48. Implications on the design of 3D printed electronics to facilitate the incorporation of these methods in the recycling process are discussed on page 44.

The results of this exploration of methods suggest that the most promising method to release silver circuitry from PLA substrate is to heat the substrate and circuitry by submerging the object in near-boiling water and moving the circuitry and substrate relatively to each other.

Ultrasound was investigated as a method to induce this relative movement in the product while it is submerged in hot water. This method shows promising results, but needs further investigation before conclusions can be drawn on applicability of this method.

The simulations showed that electromagnetic induction of currents through the silver tracks, within the limits of this study, would be far too low to be able to let them release from the substrate in the proposed way. The current was so low that can be concluded that inductive heating of embedded circuitry will not be a feasible method even with adjusted dimensions and different materials.

The use of contact electrodes to apply high current to the silver tracks did partially achieve the desired result. It was assumed that this approach could not be used in an economically feasible way on an industrial scale, and thus was not further investigated as a method on its own. Perhaps this decision can be reviewed, or other methods of application of high current can be investigated in further research.

Based on the results of experiments with microwaves it can be argued that microwaves cannot be used for the intended purpose within the limitations set in this explorative research. With advancements in the technology that lead to uniform deposition of the circuitry and improved control over the power and distribution of the microwaves, this method might prove better applicability in the future.

Implications for design of 3D printed electronics.

The promising results of tests with samples submerged in the hot water, can lead to implementation of a similar process in practice. To be able to be treated like this in a recycling process, requirements need to be met in the design of 3D printed electronics, but different approaches can be taken to enable the use of the discovered principle.

To be able to implement the heat based method, heat needs to be able to reach the substrate near the circuit. This can be achieved by exposing the circuits, for instance by integrating design for liberation measures as discussed earlier in the report (page 32). As noted in that chapter, printing large parts of the circuit in an x-y plane facilitates the exposure of the circuits, as fracture in the x-y plane realized the best results with the tested alterations. Measures to guide selective fracture in other directions of the products can be used to expose (parts of the) circuit too. Although the success rate of those alterations was lower in the experiments in this study, they do allow for more freedom in the design of 3D printed electronics.

In the conducted experiments samples with external circuits were treated with hot water. However, the heat can be applied through hot air too, and applications can be designed in which the heat is enabled to reach internal parts of the product. Heat can also reach the required parts of the product if they are not exposed, for instance through liquid that can flow through the product and is allowed to reach all parts of the circuit. This can for instance be enabled by optimizing the size of the head spaces above the circuit, integration of channels that can act as flow leaders through the product, or the integration of capillary structures in the voids around the printed circuit. Selective fracturing in a consecutive shredding process will still be needed to liberate the released silver from the product.

Another requirement that follows from the implementation of such a process in practice is that the 3D printed electronics should allow for relative movement between the substrate and circuit after heating. When exposing of the circuit is enabled, this relative movement can be induced by external sources such as a brush that sweeps over the circuit, or several pieces of substrate with circuitry attached that slide over each other as they are submerged in the hot liquid together.

The explored method of ultrasound treatment can be used to induce this relative movement. This method does require the circuit to be exposed, which can be achieved through incorporation of the aforementioned design for liberation measures in the design. This method of inducing relative movement with ultrasounds combines well with the submersion of a products in hot liquid.

Another possible way to enable this relative movement is by allowing the substrate layers on which the silver is deposited to bend when the material is softened. This can either be achieved by avoiding structures that remain rigid when the material is softened by heat, allowing the structure to bend under its own weight, or by incorporating structures in the product that will deform when heated through for instance differences in thermal expansion.

The results of the experiments with microwaves and induction in this research were, in terms of successfully released silver, unsatisfactory to such an extent that no vision on the implications on the design of 3D printed electronics can be given, because the results do not forecast a successful implementation of one of these methods in any form.



Figure 63: Silver bits retrieved from the samples used in the experiments. Approximately 2,1 grams.

PRELIMINARY SCHEMATIC GUIDELINES FOR RECYCLABLE 3D PRINTED ELECTRONICS

Based on the results of the both the explorative study into methods to release silver circuitry from a PLA substrate and the study on design for liberation measures for 3D printed objects, a flow diagram has been derived to offer guidelines to improve recyclability. The flow diagram in figure 64 leads a designer to one of five recycling scenarios based on key characteristics of the designed product. This scenario is a description of the recycling process that leads to the highest yield of metal recovery with the lowest amount of steps in the process, to account for economical viability of the process. For each scenario a set of guidelines is drafted based on the results of this project.

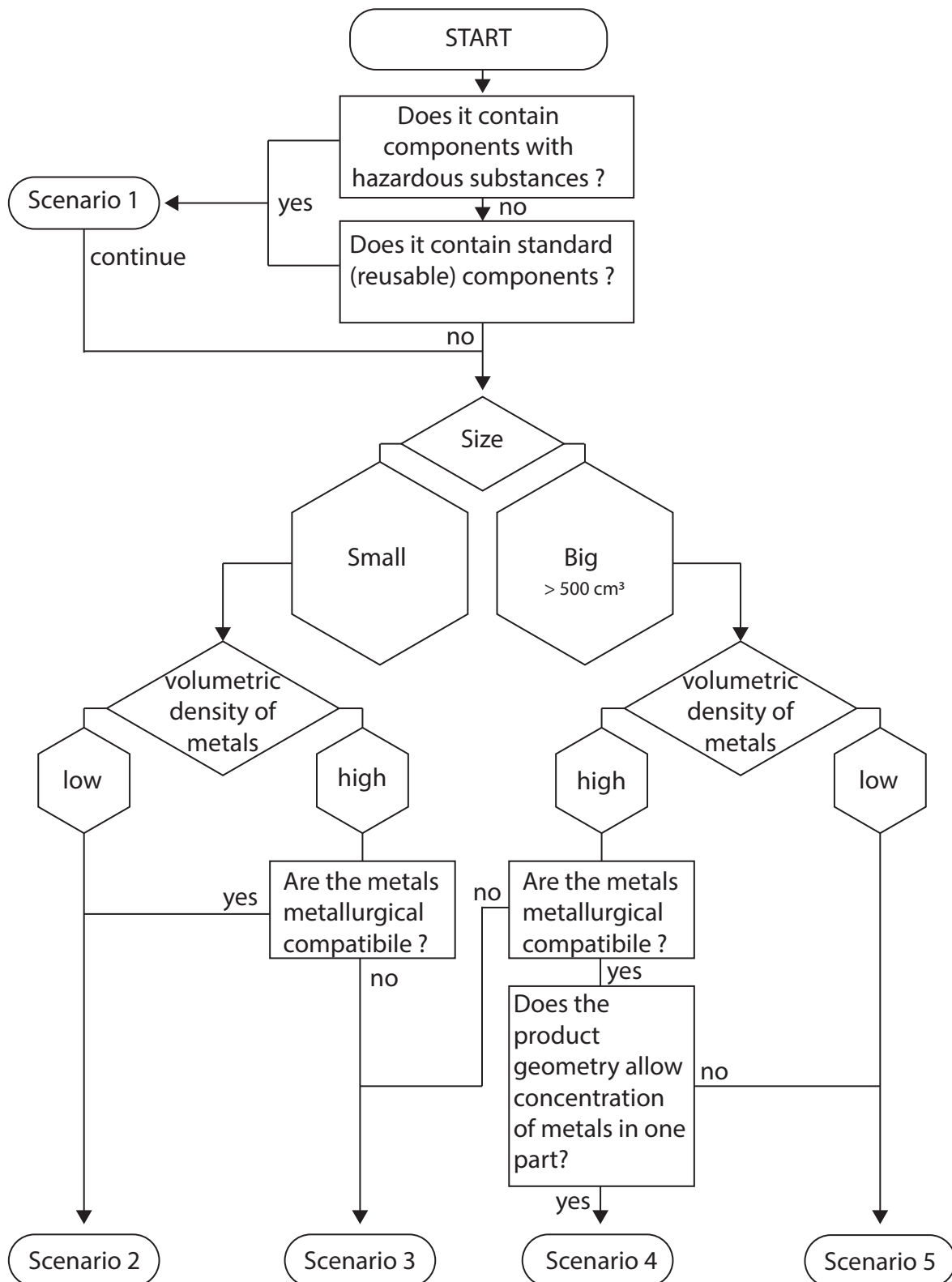


Figure 64: Flow diagram directing to recycling scenarios with design guidelines.

Scenario 1:

Valuable, reusable components or components of the product that contain hazardous substances that should not be shredded, as discussed on page 7, should be taken out in the dismantling stage of the recycling process.

To facilitate dismantling by design, the measures proposed to enable liberation of materials in a shredder should be adapted to make break-away structures for (manual) disassembly that enable the selective removal of components, as discussed on page 30. For instance creating weaknesses in the layers above voids where the components are placed in.

Besides the guideline to facilitate dismantling, the designer should incorporate other guidelines based on other product characteristics by continuing through the flow diagram.

Scenario 3:

Products with a high volumetric density of metallurgical incompatible metals will most economically be processed by liberating the dissimilar materials in a fine shredding process after which the metals can be separated by electrostatic separation, or magnetic separation when ferrous metals are involved, to have the separate fractions pyrometallurgically refined, or when a fraction of only Ag, Au or Pt is left hydrometallurgically refined.

When a significant amount of a metal is (economically) unrecoverable in the chosen metallurgical process, separation of the concerned metals should be incorporated in the design of the product. This is facilitated by incorporating spacing or break-away structures between the deposited metals that will make them separate in a shredder, as discussed on page 32.

Another solution is to enable hot liquid treatment of the circuitry locally in the part of the product where the metallurgically incompatible metals meet as described on page 44. To facilitate this treatment the circuits should be exposed by integrating design for liberation alterations as discussed on page 32, or by facilitating flow of hot liquid through the product near the circuits as discussed on page 44.

The above described guidelines allow both pyrometallurgical as hydrometallurgical refining.

Scenario 2:

Small products with a high volumetric density of metallurgical compatible metals, or small products with a low volumetric density of metals, will probably most economically be processed when they are integrally send to a smelter for pyrometallurgical refining.

No specific guidelines for 3D printed electronics have to be taken into account, but limit the amount of metal that are lost in the slag.

When the designer knows the product will be processed through the hydrometallurgical route, continue to scenario 5.

Scenario 4:

Bigger products with a high volumetric density of metallurgical compatible metals will most economically be processed by removing the redundant substrate parts by coarse shredding and refining the leftover parts with concentrated metal density through the pyrometallurgical route. When the metals are concentrated and have a volumetric percentage above 7% the metal containing parts can be separated from the non-metal containing parts by density separation (as calculated in box 1 on page 8). To improve efficiency of the refining process concentrate the metals in parts of the product that can be liberated by breaking off redundant substrate parts in a coarse shredder.

Liberation of specific metal containing parts is facilitated in design by incorporating measures for guided fracturing in a shredder as discussed on page 32. When the designer knows the metals will be refined in a hydrometallurgical process, continue to scenario 5.

Scenario 5:

Big products with a low volumetric density of metals will most economically be recycled by liberating the metals in a shredding process after which the dissimilar materials can be separated by density separation, or magnetic separation when ferrous metals are involved, to have the metals hydro- or pyrometallurgically refined.

To facilitate density separation, the metals must be well liberated from the substrate. Treatment with hot liquid can be used to weaken the bond between circuitry and substrate as described on page 44.

To facilitate this treatment the circuits should be exposed by integrating design for liberation alterations as discussed on page 32, or by facilitating flow of hot liquid through the product near the circuits as discussed on page 44.

An additional flow chart (figure 65) is made that shows the suggested recycling processes that have led to the guidelines as proposed in this chapter. In the diagram the product characteristics used in the first diagram lead to recycling methods shown in rounded rectangles with the corresponding design guidelines shown in hexagons. Recycling methods proposed in the diagram are chosen to lead to the highest yield of metal recovery with the lowest amount of steps in the recycling process. In the diagram the focus is on the recovery of metals, after shredding fractions of liberated (plastic) substrate are left out of the diagram.

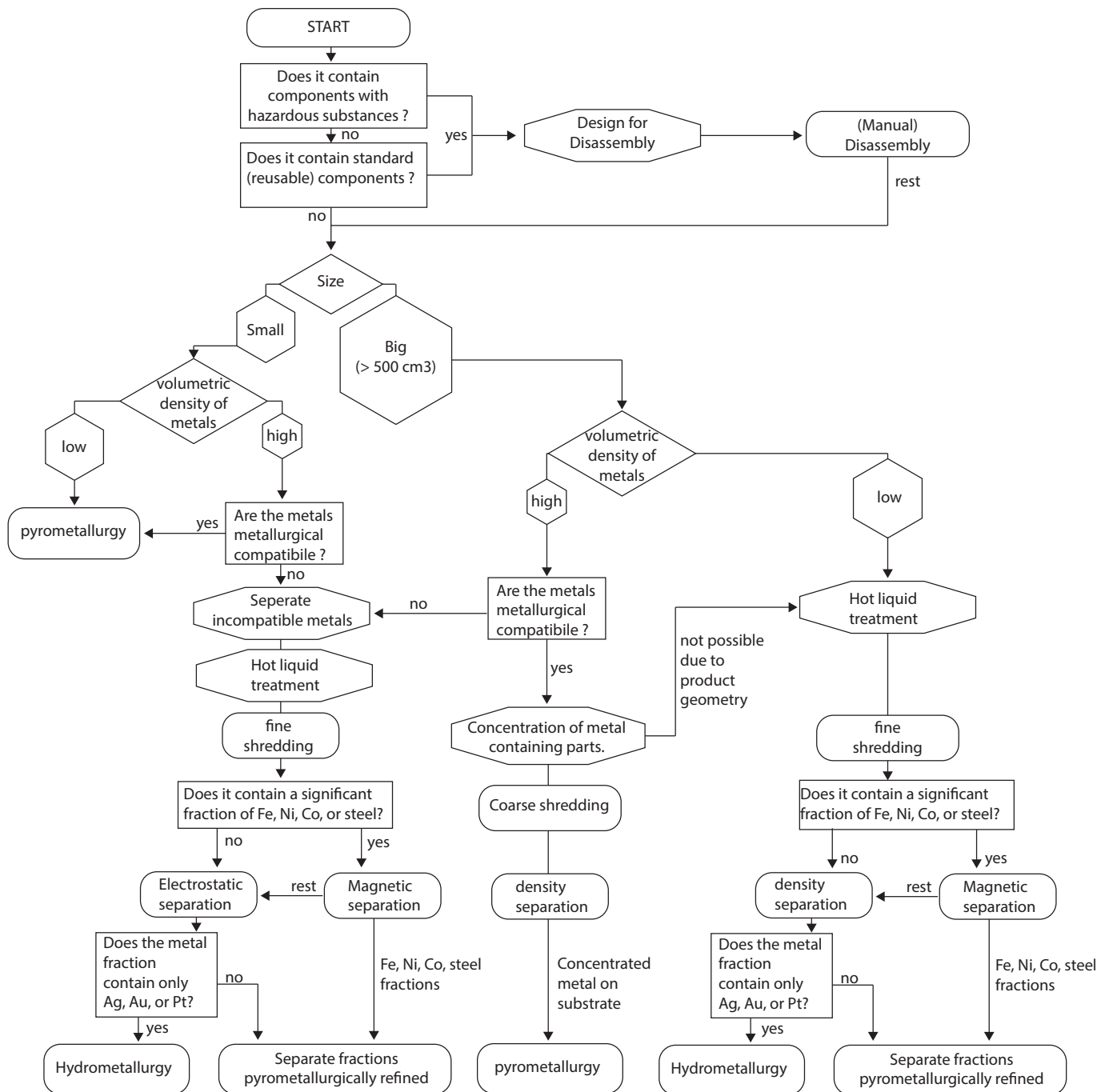


Figure 65: summarizing flow diagram that proposes the most economical recycling processes and corresponding design guidelines, as discussed in this chapter.

RECOMMENDATIONS FOR FURTHER RESEARCH

To the best of my knowledge, the two-part explorative research discussed in this thesis are the first studies on the specific topic of recycling of 3D printed electronics. The results of the two studies show possible solutions to solve the identified problems, but raise questions too. Questions prompted but left unsettled by these studies can be used as the inception for further research that might lead to elaboration of the guidelines for recyclable 3D printed electronics or new methods that will aid in the recycling process. In this chapter several potential subjects for further research are discussed.

Design for liberation of 3D printed electronics

In the performed research on liberation measures in 3D printed objects, the focus was put on how the objects would break and only slightly on how the alterations impact the strength of the structures. A more extensive strength analysis of the proposed structures should be performed to determine how these impact the lifespan of products during normal, day-to-day, use.

Conclusions drawn from the experiments focus on the fracture of the objects in planes mainly. One of the key benefits of 3D printing as a production technique is the advanced freedom in design to create oddly shaped structures. More research could be done in the guided fracture of 3D printed objects around oddly shaped forms.

This project focussed on the liberation of circuitry off of a substrate, more specifically the release of silver from PLA. Electronics involve more than just circuitry, future studies could look into the dismantling of electronics to release components for reuse or further processing.

A decision was made to look into the destructive disintegration of products in the recycling process to liberate materials. Another study could look into the non-destructive disassembly of 3D printed electronics to retain more value in products and components in a circular economy.

Ultrasounds

The tests with an ultrasonic cleaner show promising results in inducing relative movement between the circuitry and substrate and releasing silver. This method could be used relatively easy on a larger scale but the yielded percentages of released silver lack behind on the results of the other experiments with hot water but without ultrasounds. These experiments showed that the best results were obtained at higher temperatures that could not be reached in the experiments with ultrasounds. The used ultrasonic cleaner was limited in its frequency to a fixed 42 kHz, while a lower frequency could be used to generate more powerful forces in the fluid (Ensminger & Bond, 2011). In a future study the results of higher fluid temperatures, lower frequencies, or a combination of the two, could be investigated.

It was not recorded at what time the circuit released from the substrate in the ultrasonic cleaner and it could not be concluded whether the release percentage was time dependent. In a future research optimization of treatment time could be investigated.

Microwave

For the experiments to determine the feasibility of the use of microwaves to liberate silver from PLA, a common consumer grade microwave oven, limited in adjustability and accuracy, was used. A follow-up study committed to the feasibility of the use of microwaves for this purpose, should be able to find more accurate results when transmitted power, time of exposure, and distribution of the microwaves through the sample are controlled.

Induction

Although ruled out as a method applicable on larger scale early in this explorative research, the use of contact electrodes can be further investigated: are there possibly ways to apply high current to partially opened tracks in a large scale operation?

Boiling tests:

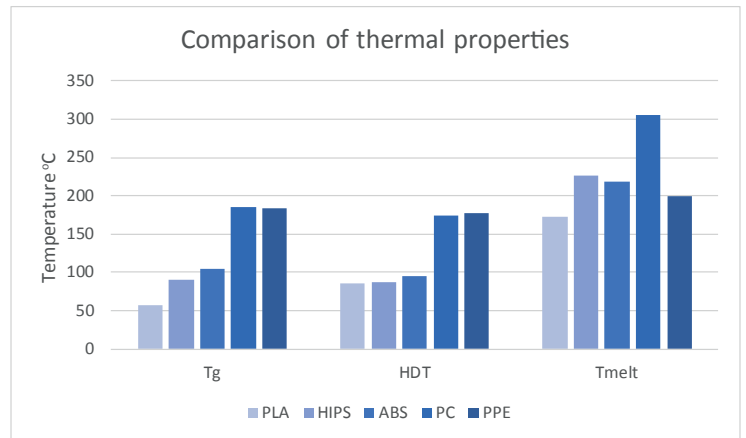
During the experiments in which samples were submerged in hot water, the temperature of the water varied between 66 °C and 98 °C. The results of this small number of experiments did not indicate a significant relation between a higher temperature and higher release rate. When a similar method is applied on an industrial scale, for economical reasons a trade-off will need to be made between a lowest possible temperature, shortest possible processing time, and highest yield of retrieved silver. A study should be conducted to find the most optimal conditions.

In this explorative study it was found that the substrate and silver had to be moved relative to each other during or shortly after the immersion in hot water. A follow-up research can look into methods to reach this goal that are suitable to be used on industrial scale in a recycling facility.

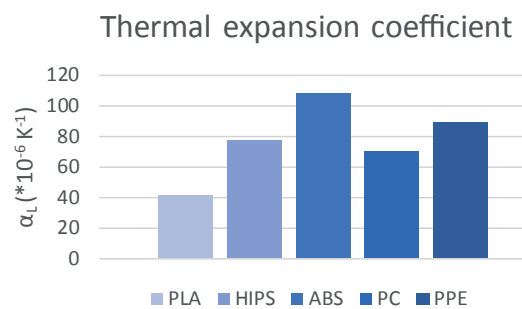
Moreover, it might be possible to design measures that allow for the spreading of hot liquid or movement of the substrate in this part of the recycling process into the 3D printed products. These measures could be studied, in the same way as measures to allow for improved liberation in a shredder were studied in this project.

The results of this study show that submerging samples in hot water yields the best results between the compared methods. However, others methods to uniformly heat 3D printed objects above the glass transition temperature of the substrate material can still be researched for comparison, for instance heating the objects with hot air.

The method proved successful for the material combination of the chosen samples, PLA and silver. However, consumer electronics are commonly not produced from these materials, or not in the combination of just these two materials. Plastics commonly used in the embodiment of electronics tend to have a higher glass transition temperature and melting point, and other thermal properties, see graphs 3 & 4. For application in the recycling of consumer grade 3D printed electronics, studies should be done into the behaviour of other material combinations treated in a similar way, and whether other hot liquids should be used for this.



Graph 3: A comparison of thermal properties of PLA and the four most commonly used thermoplastics in electronics: HIPS, ABS, PPE, and PC (Kang & Schoenung, 2005; Babu, Parande, and Basha, 2007; Wäger & Hischer, 2017). The compared properties are glass transition temperature (Tg), heat distortion temperature (HDT), and melting temperature (Tmelt). Values are retrieved from the Cambridge Engineer Selector (version 17.1.0, Granta Design Limited, 2017).



Graph 4: A comparison of thermal expansion coefficients of PLA, HIPS, ABS, PPE, and PC. Values are retrieved from the Cambridge Engineer Selector (version 17.1.0, Granta Design Limited, 2017).

Figure 66: 3D printed turtle shaped samples used in the experimental work of this thesis arranged: the top three samples are unaffected, the next four have been used in the microwave experiments (see page 38). The next one has lost some silver in the ultrasonic cleaner (see page 42), from the last five samples almost all circuitry was released in the experiments with hot water (page 40). Some of the retrieved silver circuitry has been laid out on the left of the samples.



ACKNOWLEDGEMENTS

I would like to extend my gratitude to my supervisory team, Yu Song and Ruud Balkenende, for giving me the opportunity to graduate on this topic, for their guidance, for sharing their knowledge and ideas with me, and for their enthusiasm while supervising this graduation project.

I would like to acknowledge and thank Tao Hou for his contributions to this thesis by providing his support and explanation of electromagnetic induction and performing the induction simulations as described on page 35.

I would like to express my appreciation for the support received with the practical experiments at the TU Delft by:
Mascha Slingerland at the Applied Labs at the faculty of Industrial Design Engineering.
Peter Berkhout at the Resources & Recycling labs at the faculty of Civil Engineering and Geosciences.
Tino Kool at the Quantum Nanoscience lab at the faculty of Applied Sciences.

I am obliged to Mariska Maas and Song-Chuan Zhao for providing me with samples of 3D printed electronics.

Lastly, I would like to thank Jasper Barsingerhorn for proofreading this thesis.

REFERENCES

- Akcil, A., Erust, C., Gahan, C. S., Ozgun, M., Sahin, M., & Tuncuk, A. (2015). Precious metal recovery from waste printed circuit boards using cyanide and non-cyanide lixiviants—a review. *Waste Management*, 45, 258-271.
- Ansys Inc (2015). Ansoft Maxwell [computer software]. Canonsburg, ANSYS Inc.
- Ansys Inc (2017). Ansys Workbench 18.2 [computer software]. Canonsburg, ANSYS Inc.
- Babu, B. R., Parande, A. K., & Basha, C. A. (2007). Electrical and electronic waste: a global environmental problem. *Waste Management & Research*, 25(4), 307-318.
- Bailey, C., Stoyanov, S., Tilford, T., & Tourloukis, G. (2017, April). 3D & printed electronics manufacturing strategies. In *Electronics Packaging (ICEP), 2017 International Conference on* (pp. 312-315). IEEE. Retrieved from: <http://ieeexplore.ieee.org/abstract/document/7939383/>
- Baldé, C.P., Forti V., Gray, V., Kuehr, R., Stegmann, P. : The Global E-waste Monitor – 2017, United Nations University (UNU), International Telecommunication Union (ITU) & International Solid Waste Association (ISWA), Bonn/Geneva/Vienna.
- Baldé, C.P., Wang, F., Kuehr, R., Huisman, J. (2015), The global e-waste monitor – 2014, United Nations University, IAS – SCYCLE, Bonn, Germany. <https://i.unu.edu/media/unu.edu/news/52624/UNU-1stGlobal-E-Waste-Monitor-2014-small.pdf>
- Balkenende, R. (2013). Design for Recycling applied to LED-lamps. VTT Webinar, retrieved from http://www.vtt.fi/Documents/vtt_webinar_ruud_balkenende.pdf
- Boekraad, R. (2017). 3D Printed Electronics: a case study on Wireless Power Transfer. (Master thesis) Retrieved from: <https://repository.tudelft.nl/islandora/object/uuid%3Ac23956ae-2abd-4a73-b172-def9cde5f159>
- Branson Ultrasonic S.A. (2007). Branson model 1510E-DTH [Ultrasonic cleaner]. https://www.branson.nl/downloads/NL_BRANSON_irl.pdf
- Brockotter, R. (2018). Key design considerations for 3D Printing. Retrieved from: <https://www.3dhubs.com/knowledge-base/key-design-considerations-3d-printing>
- Buchert, M., Manhart, A., Bleher, D., & Pingel, D. (2012). Recycling critical raw materials from waste electronic equipment. Freiburg: Öko-Institut eV, 49(0), 30-40.
- Cui, J., & Forssberg, E. (2003). Mechanical recycling of waste electric and electronic equipment: a review. *Journal of hazardous materials*, 99(3), 243-263.
- Diener, A. (2010, February 1). Afterlife: An Essential Guide To Design For Disassembly. Retrieved from <http://www.core77.com/posts/15799/afterlife-an-essential-guide-to-design-for-disassembly-by-alex-diener-15799>
- Dresher, W. H. (2004, May). Producing Copper Nature's Way: Bioleaching. Retrieved from https://www.copper.org/publications/newsletters/innovations/2004/05/producing_copper_natures_way_bioleaching.html#xmpls
- Ellen MacArthur Foundation. (2013a). Towards the Circular Economy Vol. 1 (Economic and business rationale for an accelerated transition). <https://www.ellenmacarthurfoundation.org/publications/towards-the-circular-economy-vol-1-an-economic-and-business-rationale-for-an-accelerated-transition>
- Ellen MacArthur Foundation. (2013b). Towards the Circular Economy Vol. 2 (Opportunities for the consumer goods sector). <https://www.ellenmacarthurfoundation.org/publications/towards-the-circular-economy-vol-2-opportunities-for-the-consumer-goods-sector>
- Ensminger, D., & Bond, L. J. (2011). *Ultrasonics: fundamentals, technologies, and applications*. CRC press.
- Espalin, D., Muse, D. W., MacDonald, E., & Wicker, R. B. (2014). 3D Printing multifunctionality: structures with electronics. *The International Journal of Advanced Manufacturing Technology*, 72(5-8), 963-978. Retrieved from: <https://link.springer.com/content/pdf/10.1007%2Fs00170-014-5717-7.pdf>
- EU directive on WEEE. (2012). Directive 2012/19/EU of the European Parliament and of the council of 4 July 2012 on waste electrical and electronic equipment. Retrieved from <http://eur-lex.europa.eu/legal-content/en/TXT/?uri=CELEX:32012L0019>
- Gao, W., Zhang, Y., Ramanujan, D., Ramani, K., Chen, Y., Williams, C. B., ... & Zavattieri, P. D. (2015). The status, challenges, and future of additive manufacturing in engineering. *Computer-Aided Design*, 69, 65-89. Retrieved from: <https://www.sciencedirect.com/science/article/pii/S0010448515000469>
- Goosey, M., & Kellner, R. (2002). A scoping study: end-of life printed circuit boards. Intellect and the Department of Trade and Industry.
- Gramatyka, P., Nowosielski, R., & Sakiewicz, P. (2007). Recycling of waste electrical and electronic equipment. *Journal of Achievements in Materials and Manufacturing Engineering*, 20(1-2), 535-538.
- Granta Design Limited. (2017). *Cambridge Engineering Selector* (Version 17.1.0). Cambridge, United Kingdom.
- Guo, C., Wang, H., Liang, W., Fu, J., & Yi, X. (2011). Liberation characteristic and physical separation of printed circuit board (PCB). *Waste management*, 31(9), 2161-2166.
- Hoerber, J., Glasschroeder, J., Pfeffer, M., Schilp, J., Zaeh, M., & Franke, J. (2014). Approaches for additive manufacturing of 3D electronic applications. *Procedia CIRP*, 17, 806-811. Retrieved from: <https://www.sciencedirect.com/science/article/pii/S2212827114003424>
- Hultgren, N. (2012). Guidelines and Design Strategies for Improved Product Recyclability-How to Increase the Recyclability of Consumer Electronics and Domestic Appliances through Product Design.
- Jennings, A. (2017, December). 3D Printing Troubleshooting: 34 Common 3D Printing Problems. Retrieved from: <https://all3dp.com/1/common-3d-printing-problems-troubleshooting-3d-printer-issues/>
- Kang, H. Y., & Schoenung, J. M. (2005). Electronic waste recycling: A review of US infrastructure and technology options. *Resources, Conservation and Recycling*, 45(4), 368-400.

- Kantola, V., Kulovesi, J., Lahti, L., Lin, R., Zavodchikova, M., & Coatanéa, E. (2009). Printed Electronics, Now and Future. In *Bit bang – rays to the future*. (pp. 63-102). Aalto University School of science and technology. [https://tutcris.tut.fi/portal/en/publications/printed-electronics-now-and-future\(332d4b5d-cd6a-4e14-903a-e19a19f42889\).html](https://tutcris.tut.fi/portal/en/publications/printed-electronics-now-and-future(332d4b5d-cd6a-4e14-903a-e19a19f42889).html)
- Kaya, M. (2016). Recovery of metals and nonmetals from electronic waste by physical and chemical recycling processes. *Waste Management*, 57, 64-90.
- Khazaaal, M. H., & Abdulbaqi, I. M. (2016, May). Modelling, design and analysis of an induction heating coil for brazing process using FEM. In *Multidisciplinary in IT and Communication Science and Applications (AIC-MITCSA), AI-Sadeq International Conference on* (pp. 1-6). IEEE.
- Kumar, A., Holuszko, M., & Espinosa, D. C. R. (2017). E-waste: an overview on generation, collection, legislation and recycling practices. *Resources, Conservation and Recycling*, 122, 32-42.
- Li, J., Lu, H., Guo, J., Xu, Z., & Zhou, Y. (2007). Recycle technology for recovering resources and products from waste printed circuit boards. *Environmental science & technology*, 41(6), 1995-2000.
- Li, J., Shrivastava, P., Gao, Z., & Zhang, H. C. (2004). Printed circuit board recycling: a state-of-the-art survey. *IEEE transactions on electronics packaging manufacturing*, 27(1), 33-42.
- Lu, Y., & Xu, Z. (2016). Precious metals recovery from waste printed circuit boards: a review for current status and perspective. *Resources, Conservation and Recycling*, 113, 28-39.
- Lungu, M., 2009. Separation of small nonferrous particles using a two successive steps eddycurrent separator with permanent magnets, *Int. J. Miner. Pcess.*, Vol. 93, pp. 172-178.
- Maas, M. (2017). A Robot out of a 3D printer; An exploration of 3D Printed Thermal Activators. (Master thesis)
- MacDonald, E., & Wicker, R. (2016). Multiprocess 3D printing for increasing component functionality. *Science*, 353(6307), aaf2093. Retrieved from: <http://science.sciencemag.org/content/353/6307/aaf2093.full>
- MacDonald, E., Salas, R., Espalin, D., Perez, M., Aguilera, E., Muse, D., & Wicker, R. B. (2014). 3D printing for the rapid prototyping of structural electronics. *IEEE Access*, 2,234–242. <https://doi.org/10.1109/ACCESS.2014.2311810>
- Malone, E., & Lipson, H. (2008, January). Multi-material freeform fabrication of active systems. In *ASME 2008 9th Biennial Conference on Engineering Systems Design and Analysis* (pp. 345-353). American Society of Mechanical Engineers.
- Masanet, E., Auer, R., Tsuda, D., Barillot, T., & Baynes, A. (2002). An assessment and prioritization of "design for recycling" guidelines for plastic components. In *Electronics and the Environment, 2002 IEEE International Symposium on* (pp. 5-10). IEEE.
- Morgan Jr, S. P. (1949). Effect of surface roughness on eddy current losses at microwave frequencies. *Journal of Applied Physics*, 20(4), 352-362. Retrieved from: <https://aip.scitation.org/doi/pdf/10.1063/1.1698368>
- Movilla, N. A., Zwolinski, P., Dewulf, J., & Mathieux, F. (2016). A method for manual disassembly analysis to support the ecodesign of electronic displays. *Resources, Conservation and Recycling*, 114, 42-58.
- Namias, J. (2013). The future of electronic waste recycling in the United States: obstacles and domestic solutions. Columbia University.
- NatureWorks (2016). Ingeo Biopolymer 3D850 Technical Data Sheet. Retrieved from: <https://support.voxel8.co/hc/en-us/articles/207316053-SDS-Safety-Data-Sheets->
- Nave, C. R. (1999). Thermal Expansion Coefficients at 20C. [Data set] Georgia State University, Retrieved from: <http://hyperphysics.phy-astr.gsu.edu/hbase/Tables/thexp.html#c1>
- Ohkita, T., & Lee, S. H. (2006). Thermal degradation and biodegradability of poly (lactic acid)/corn starch biocomposites. *Journal of Applied Polymer Science*, 100(4), 3009-3017.
- Ongondo, F. O., Williams, I. D., & Cherrett, T. J. (2011). How are WEEE doing? A global review of the management of electrical and electronic wastes. *Waste management*, 31(4), 714-730. <http://www.sciencedirect.com/science/article/pii/S0956053X10005659?via%3Dihub>
- Ota H., Emaminejad S., Gao Y., Zhao A., Wu E., Challa S., Chen K., Fahad H. M., Jha A. K., Kiriya D., Gao W., Shiraki H., Morioka K., Ferguson A. R., Healy K. E., Davis R. W., Javey A. (2016). Application of 3D printing for smart objects with embedded electronic sensors and systems. *Advanced Materials Technologies*, 1(1).
- Polymer Database. (2015). heat distortion temperature. Retrieved from: <http://polymerdatabase.com/polymer%20physics/HeatDistortion.html>
- Smart Objects with Embedded Electronic Sensors and Systems. *Adv. Mater. Technol.*, 1: 1600013. <http://onlinelibrary.wiley.com/doi/10.1002/admt.201600013/pdf>
- Reuter, M. A., Hudson, C., Van Schaik, A., Heiskanen, K., Meskers, C., & Hagelüken, C. (2013). Metal recycling: Opportunities, limits, infrastructure. A Report of the Working Group on the Global Metal Flows to the International Resource Panel. Retrieved from: http://www.resourcepanel.org/file/313/download?token=JPYZF5_Q
- Rifer, W., Brody-Heine, P., Peters, A., & Linnell, J. (2009). Closing the Loop Electronics Design to Enhance Reuse/Recycling Value. Green Electronics Council. Final Report.
- Sanatgar, R. H., Campagne, C., & Nierstrasz, V. (2017). Investigation of the adhesion properties of direct 3D printing of polymers and nanocomposites on textiles: Effect of FDM printing process parameters. *Applied Surface Science*, 403, 551-563. Retrieved from: <https://www.sciencedirect.com/science/article/pii/S0169433217301137>

- SD3D. (2017) PLA Technical Datasheet [Data set]. Retrieved from: https://www.sd3d.com/wp-content/uploads/2017/06/MaterialTDS-PLA_01.pdf
- Simplify3D (2018). Print Quality Troubleshooting Guide. Retrieved from: <https://www.simplify3d.com/support/print-quality-troubleshooting/#layer-separation-and-splitting>
- Song, Y., Boekraad, R. A., Roussos, L., Kooijman, A., Wang, C. C. L., & Geraedts, J. M. P. (2017). 3D Printed electronics: opportunities and challenges from case studies. ASME 2017 International Design Engineering Technical Conferences & Computers and Information in Engineering Conference, Cleveland, Ohio, USA.
- Sun, K., Wei, T. S., Ahn, B. Y., Seo, J. Y., Dillon, S. J., & Lewis, J. A. (2013). 3D printing of interdigitated Li-Ion microbattery architectures. *Advanced Materials*, 25(33), 4539-4543. Retrieved from: <http://onlinelibrary.wiley.com/doi/10.1002/adma.201301036/full>
- Svoboda, J., & Fujita, T. (2003). Recent developments in magnetic methods of material separation. *Minerals Engineering*, 16(9), 785-792.
- Van Schaik, A. (2013). Design for recycling: rules and guidelines [presentation slides pdf] retrieved from: https://www.nvmp.nl/uploads/pdf/nieuws/2013/2013%2008%2029%20MARAS_DfR%20rules%20and%20guidelines_NVMP%20symposium_S.pdf
- Veit, H. M., Diehl, T. R., Salami, A. P., Rodrigues, J. D. S., Bernardes, A. M., & Tenório, J. A. S. (2005). Utilization of magnetic and electrostatic separation in the recycling of printed circuit boards scrap. *Waste management*, 25(1), 67-74.
- Voxel8 printers. (2017) Retrieved from <http://www.voxel8.com/printer/>
- Wäger, P. A., & Hischer, R. (2015). Life cycle assessment of post-consumer plastics production from waste electrical and electronic equipment (WEEE) treatment residues in a Central European plastics recycling plant. *Science of the Total Environment*, 529, 158-167.
- Webster, C. (2013). Engineering the Circular Economy: The art of design for disassembly.. Retrieved from https://www.ellenmacarthurfoundation.org/assets/downloads/news/EMF_Engineering-the-Circular-Economy_300913.pdf
- Wohlers, T., & Gornet, T. (2014). History of Additive Manufacturing. Wohlers Report 2014 - 3D Printing and Additive Manufacturing State of the Industry, 1-34. <https://doi.org/10.1017/CBO9781107415324.004>
- Wolfram|Alpha Knowledgebase (2018). Silver density. Retrieved from: <http://m.wolframalpha.com/input/?i=silver+density>
- Wu, J., Li, J., & Xu, Z. (2008). Electrostatic separation for recovering metals and nonmetals from waste printed circuit board: problems and improvements. *Environmental science & technology*, 42(14), 5272-5276.
- Wu, S. Y., Yang, C., Hsu, W., & Lin, L. (2015). 3D-printed microelectronics for integrated circuitry and passive wireless sensors. *Microsystems & Nanoengineering*, 1, 15013. Retrieved from: <https://www.nature.com/articles/micronano201513/>
- Yang, Y., Chen, S., Li, S., Chen, M., Chen, H., & Liu, B. (2014). Bioleaching waste printed circuit boards by *Acidithiobacillus ferrooxidans* and its kinetics aspect. *Journal of biotechnology*, 173, 24-30.
- Yazici, E. Y., Deveci, H., & Alp, I. (2010). Eddy Current Separation of Metals from E-wastes. *Proceedings of the XIIth. International Mineral Processing Symposium*, 12, 1207-1215]
- Yazici, E. Y., Deveci, H., Yazici, R., Greenway, R., & Akcil, A. (2011). Recovery of copper from scrap TV boards by eddy current separation. In *Proceedings of the 15th Conference on Environment and Mineral Processing, Part I. VSB Tech. University of Ostrava, Czech Republic* (pp. 27-33).
- ZERMA machinery and recycling technology (2018). *GSL – Slow Speed Granulators*. Retrieved from: <https://zerma.com/en/Granulators/GSL>
- Zhang, L., & Xu, Z. (2016). A review of current progress of recycling technologies for metals from waste electrical and electronic equipment. *Journal of Cleaner Production*, 127, 19-36.
- Zhang, S., Forssberg, E., Arvidson, B., and Moss, W., 1998. Aluminum recovery from electronic scrap by High-Force® eddy-current separators”, *Resources, Conservation and Recycling*, Vol. 23, pp. 225-24
- Zhang, S., Rem, P.C., and Forssberg, E., 1999. The investigation of separability of particles smaller than 5 mm by eddy current separation technology. Part I: Rotating type eddy current separators, *Magnetic and Electrical Separation*, Vol. 9, pp. 233-251.1.

APPENDIX I: PRELIMINARY FIELD STUDY OF NON-DESTRUCTIVE DISASSEMBLY

Design for non-destructive disassembly was considered as an option for the overall direction of this master thesis. Non-destructive disassembly allows the product to be repaired, refurbished, or remanufactured, retaining more value in the product than when it is recycled for its materials (Ellen MacArthur Foundation, 2013a). 3D printed objects were designed with modifications that allow for controlled manual disassembly to access parts of an object and in some cases reassembly of the object. In figures 67 & 68 two examples are shown.

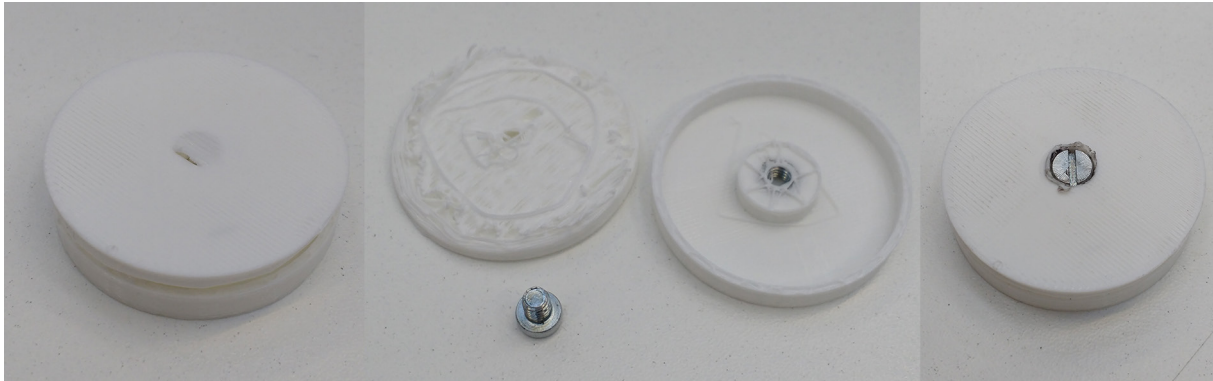


Figure 67: a 3D printed object containing an embedded screw that allows for opening and closing of the object.

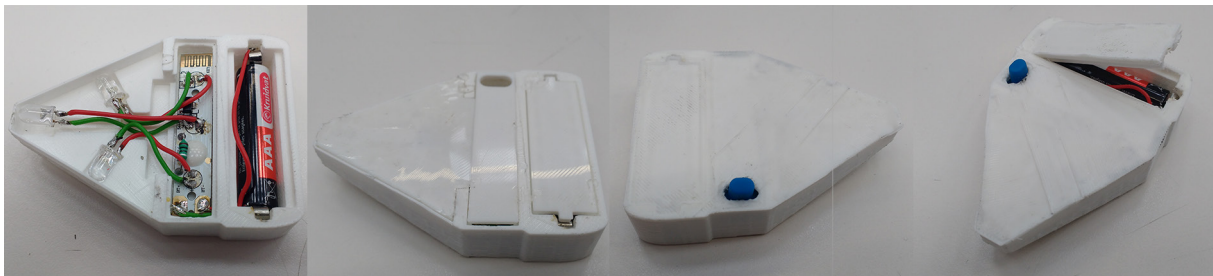


Figure 68: a 3D printed casing for a bike light with covers that can be printed over to seal the product, but can be broken open to retrieve the parts.

During the literature research into 3D printing of embedded electronics, benefits of this new production technique were found, as described on page 2. These benefits are unique strengths of this production technique that will guide in which direction this production technique will further develop and for what future applications it will be used. The defining benefit of this production technique is the advanced design freedom that is brought to the production of electronics. It allows for the fabrication of electronic circuitry in three dimensions, as opposed to the 2D planes in conventional circuit boards, and the integration of electronic components in those three dimensions and into the product (part) it is printed into. Along with this advanced integration of the electronic systems in products, this technique can be used to optimize the weight of products and product parts, or to optimize their fitting in conventionally produced products.

During the design of 3D printed objects with modifications that enable non-destructive disassembly, it was found that fasteners and local reinforcements that take up space need to be designed into products. This conflicts with the benefits of 3D printing for the miniaturization of electronics.

Furthermore, in the design guidelines for disassembly, which can be found on page 56, it is advised to split up products into separate subassemblies for maintenance to limit liability of the electronic system. However, breaking up the electronic system into subassemblies cancels the benefits of advanced integration of the electronics into the product. As the required design interventions for non-destructive disassembly oppose the core benefits of the production technique, it was decided to focus on the recycling of 3D printed electronics in the continuation of this project.

APPENDIX II: EXISTING GUIDELINES FOR DESIGN FOR DISASSEMBLY.

The following list of guidelines to improve the disassembly of conventionally produced products was compiled from literature by Rifer et al (2009), Diener (2010), Webster (2013), and Movilla et al (2016).

Materials

- Limit the amount of different materials used in a product.
- Make sure that these materials do not release toxic substances when taken apart.
- Do not mix different materials in a non-separable way (e.g. overmoulding, gluing, fusing).

Subassemblies

- Split a product up in subassemblies, to allow for repair or replacement of one subassembly without jeopardizing the components in other subassemblies.
- Do not use too many subassemblies. Each one adds to the assembly and disassembly time.

Fasteners

- Use standard fasteners such as screws with common heads to fasten parts of the product.
- Limit the number of fasteners per part to shorten assembly and disassembly time.
- Use releasable snapfits where possible to allow for shorter assembly time and (destructible) disassembly.

Information

- Indicate the used materials through markings on the parts.
- Give instructions for the proper disassembly of the product through use cues on the product.
- Give disassembly, repair, and maintenance information through written manuals.

APPENDIX III: EXISTING GUIDELINES FOR DESIGN FOR RECYCLING

As is discussed on page 7, several methods for the recycling of electronics are put in practice. Recycling methods are adopted to effectively recycle the electronics that enter the recycling stream. Generally, the recycling methods are adapted to suit the production methods and not the other way around. However, some design interventions can be taken into account to improve the recyclability of electronics. Prior to reducing the electronics into shreds, (manual) disassembly of valuable or hazardous parts is needed in the recycling process. Therefore some design guidelines that apply to Design for Disassembly (page 56), are valid for Design for Recycling too.

Materials

- Limit the amount of different materials in the product.
- Prevent the release of toxic substance in the disassembly and shredding process.
- Do not mix different materials in a non-separable way (e.g. over-moulding or metallization)

Metals:

- Metals that are non-compatible in remelting and refining should not be fastened together.

Plastics:

- Indicate materials through markings on plastic parts.
- Do not paint small (<25 gram) plastic components, to minimize effects of the paint on the recycled material in aesthetics and mechanical properties.
- Prevent (where possible) the use of filled plastics.

Connections and fasteners

- Limit the use of mechanical fasteners such as screws, pins, and rivets.
- Use snap fit connections as fasteners where possible.
- Minimize the use of glues, adhesives, and welds when connecting electronic components to structural components in the product.

Reinforcements

- The following guidelines are aimed at creating pieces of uniform composition and size when shredding for post-processing.
- Limit the incorporation of local reinforcements (such as gussets and bosses for screw threads).
- Stiff, brittle structures are preferred, as strong flexible structures tend to fold around other components in shredders.

Electronics

- Integrate as much of the electronics as possible in one piece that can be taken out of the product in pre-processing before shredding.
- SMD (surface mounted device) connections are preferred over wire connections.

This list of guidelines was compiled from literature by Masanet et al (2002), Rifer et al (2009), Diener (2010), Hultgren (2012), and Balkenende (2013).

APPENDIX IV: PRELIMINARY SHREDDER TESTS

Liberation of silver tracks off of the PLA substrate in a shredder was tested by shredding three batches of randomly chosen samples in a cutting mill with three different sieves. The sieves had holes of respectively 8, 6, and 4 mm, determining the maximum diameter size of the shreds that are allowed to pass. Samples were obtained from graduation research (Maas, 2017) into 3D printed electronics and manufactured with a Voxel8 multi-material printer.

After shredding the silver and PLA shreds were separated using a two stage salt water density separation method. The density of the used PLA is $1,24 \cdot 10^3 \text{ kg/m}^3$ (NatureWorks, 2016) and the density of the silver was estimated to be $10,49 \cdot 10^3 \text{ kg/m}^3$ as this is the density of regular silver (WolframAlpha Knowledgebase, 2018), thus water with an approximate salinity of 26% was chosen as this has a density of $1,26 \cdot 10^3 \text{ kg/m}^3$. The mixture of shreds was immersed in this water, this separated the fraction of the mixture consisting of large shreds of PLA. The sunken rest of the shreds was immersed again in a salt water mixture with a salinity of approximately 32%, and stirred. This separated the shred mixture in two parts: one consisting of the smallest debris, and one of middlings of PLA and silver, and the released silver debris. This last mixture of shreds was separated manually. The final result were four separate fractions: substrate shreds, silver traces, middling shreds, and a mixture of small PLA and silver debris. An example of these four fractions is shown in figure 69. The mixture of each batch was separated, and each resulting fraction was weighed. The scales used had a resolution of 0,1 gram. The result can be found in table 13.

Size →	< 8 mm	< 6 mm	< 4 mm
Fraction ↓	Weight in grams		
Substrate	4,1	3,2	3,8
Middlings	1,3	1,6	0,6
Silver	0,1	0,2	0,2
Debris mix	0,6	0,8	0,8

Table 13: results preliminary shredder tests.

From the numbers in the table it can be observed that liberation of materials is not satisfactory in any of these cases. The goal is to retrieve the silver from the samples and it is presumed that traces of silver are left in all fractions except the substrate fraction. The middlings are in the fraction in which the silver did not release from the substrate, the fraction of mixed debris seems to be liberated and might be further separated in a more controlled process. The weight percentage of the middlings in the silver containing fraction can be calculated per used sieve size, the results are shown in table 14

	< 8 mm	< 6 mm	< 4 mm
% middlings in silver containing fractions	65,0	61,5	37,5

Table 14: percentage of middlings in the silver containing fraction per sieve size.

It shows that with decreased sieve size, the percentage of middlings decreases too. However, a percentage of almost 40% of middlings shows that with the smallest tested sieve size the release of silver is not sufficient.

It should be noted that the samples per batch were chosen at random without documenting their specifics. Variations in percentages of silver used on the samples could have influenced the result of the absolute released silver, but not the percentages of middlings to released silver.

Small traces of silver could still have been attached to the substrate separated in the substrate fraction. These traces must have been so small in weight percentage that they ended up in this fraction, but will count as losses in a recycling process.

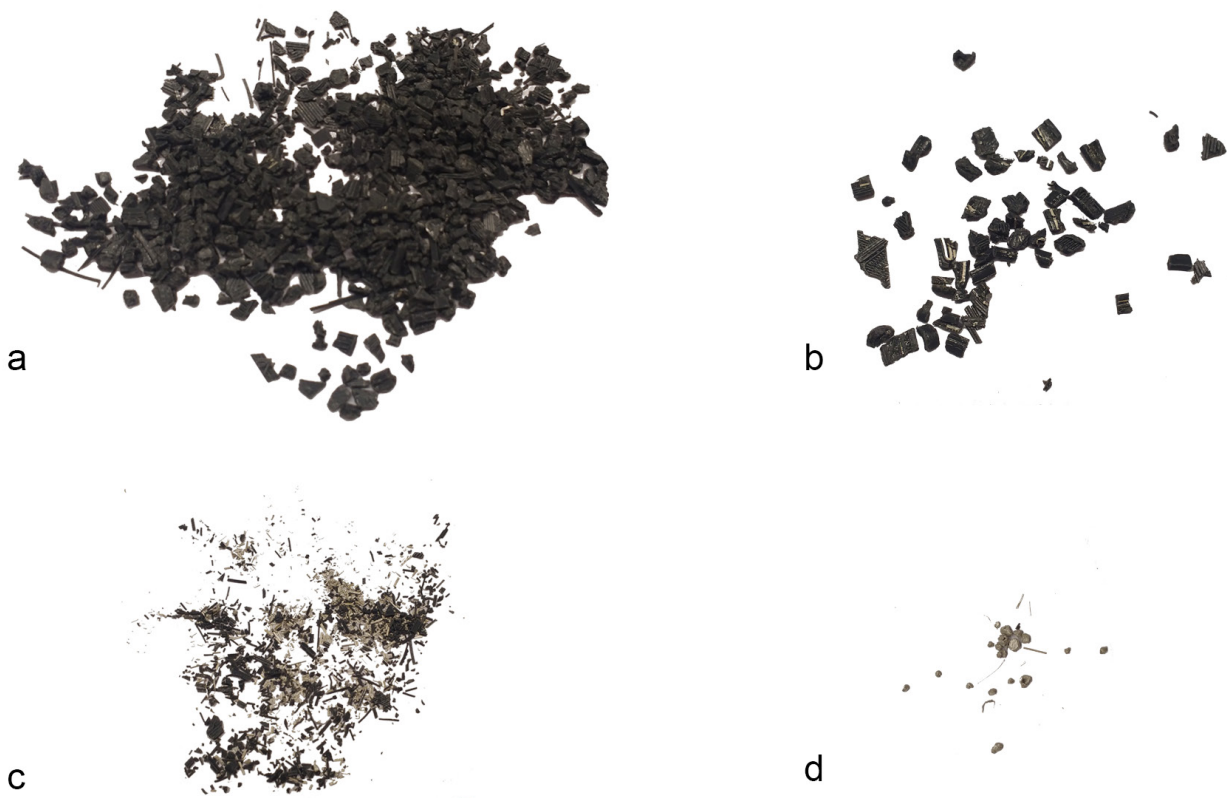


Figure 69: separated fractions of shredding with a <4 mm sieve: a) substrate, b) middlings, c) debris mix, d) silver.

APPENDIX V: RESULTS DESIGN FOR LIBERATION TESTS

layer adhesion (z-direction)	shape	visibility	strength	release	simplicity	shredded	shred result
<i>double height</i>							
0.1 to 0.2 x1	cube	5	5	1	5	no	
0.15 to 0.3 x1	cube	5	5	2	5	yes	0/3
0.2 to 0.4 x1	cube	4	4	3	5	no	
0.3 to 0.6 x1	cube	2	3	3	5	no	
<i>triple height</i>							
0.1 to 0.3 x1	cube	3	4	2	5	no	
0.2 to 0.6 x1	cube	3	5	2	5	no	
<i>half height</i>							
0.2 to 0.1 x1	cube	5	5	2	5	yes	0/3
0.2 to 0.1 x2	cube	5	5	2	5	yes	0/4
0.2 to 0.1 x4	cube	4	5	3	4	yes	2/4
0.2 to 0.1 x8	cube	3	5	4	4	yes	2/3
0.3 to 0.15 x2	cube	5	3	1	5	yes	0/3
0.3 to 0.15 x4	cube	3	2	3	4	yes	1/3
0.4 to 0.2 x1	cube	5	1	2	5	no	
<i>remove fill layer</i>							
0.15 -1	round tube	5	5	1	5	no	
0.2 -2	round tube	5	5	3	5	no	
0.2 -3	round tube	5	5	3	5	yes	1/3
0.2 x2: -1,1,-1	round tube	5	5	1	5	no	
0.2 x3: -1,1,-1,1,-1	round tube	5	4	3	5	yes	0/3
<i>change fill layers</i>							
triangle to grid x3	round tube	2	5	2	3	yes	0/3
triangle to concentric x3 ^	round tube	3	5	5	3	yes	2/3
honeycomb to grid x3	round tube	5	5	4	3	yes	3/5
honeycomb to grid x4	round tube	5	5	5	3	yes	2/5
honeycomb to concentric x3 ^	round tube	5	5	4	3	yes	3/5
grid to line x3	round tube	3	5	2	3	yes	0/3
grid to concentric x3	round tube	5	5	4	3	yes	2/3
<i>shell lines</i>							
3 to 2 *^	cube	5	5	2	4	no	
3 to 1 *^	cube	4	3	4	4	no	
2 to 1 *^	cube	4	5	3	4	no	
<i>combined</i>							
L0.2to0.1, honeyc to grid, S2to1 x6	octagonal tube	3	5	5	3	yes	2/3
L0.2to0.1, honeyc to conc, S2to1 x6	octagonal tube	3	5	5	3	yes	3/3
L0.2to0.1, grid to conc, S3to1 x3 ^	octagonal tube	4	5	-	3	only	0/3
L0.2to0.1, grid to conc, S3to1 x6 ^	octagonal tube	3	5	-	3	only	2/3
remarks:							
nozzle diameter is always 0.4, material is always PLA (jupiter series 123-3D), mostly white 2.85 mm, *= black 1.75mm, infill percentage mostly 10%, ^=15%							
All cubes were 30x30x30mm cubes, the round and octagonal tubes were 40 mm wide by 60mm tall, the triangles were 10 mm high and had even sides of 50 mm.							
In the test with the double walls, the Shred Result number is the amount of (almost) complete cubes that could be liberated in the shredder.							

Vertical fracture lines (x-or y-direction)	shape	visibility	strength	release	simplicity	shredded	shred result
<i>in walls</i>							
30 degree 80% cut inner walls in 1 plane	flat triangle	5	3	5	4	no	
45 degree 50% cut inner walls in 1 plane	flat triangle	5	4	4	4	yes	3/6
45 degree 50% cut inner walls in 2 planes	flat triangle	5	4	4	3	yes	2/6
1mm straight 50% cut inner wall in 2 planes ^	cube	5	5	4	3	yes	1/3
2mm straight 50% cut inner wall in 2 planes ^	cube	4	4	5	2	yes	2/3
<i>cross sectional</i>							
1mm cross sectional cuts with walls.	cube	5	5	4	5	yes	2/4
2mm cross sectional cuts without walls ^	cube	5	4	5	2	yes	3/3
2mm cross sectional airgaps with walls.	octagonal tube	5	5	-	4	only	0/3
curved cut (max. 3mm) with walls in 1 plane	octagonal tube	5	4	-	5	only	2/4
1mm diagonal cut + hollow corners ^	cube	5	5	-	5	only	1/3
8x 2mm cross sectional cuts with walls ^	octagonal tube	5	3	-	5	only	3/3
averting breaks							
<i>double walls</i>							
2x 0.4 mm walls with 0.4 mm space	cube in hexagonal tube	5	5	-	3	only	0/3
2x 0.6 mm walls with 0.4 mm space	cube in hexagonal tube	5	5	-	3	only	1/3
2x 0.6 mm walls with 0.7 mm space	cube in hexagonal tube	5	5	-	3	only	0/3
2x 0.4 mm walls with 0.7 mm space	cube in hexagonal tube	5	5	-	3	only	2/3
<i>infill</i>							
15% honeycomb cube in grid 5%	cube in hexagonal tube	5	5	-	1	only	0/3
15% honeycomb cube in concentric 10% ^	cube in hexagonal tube	5	5	-	1	only	0/3
15% triangular cube in concentric 10% ^	cube in hexagonal tube	5	5	-	1	only	0/3
combining strengths and weaknesses to release inner shapes							
<i>watch shapes</i>							
0.4 mm double walls + 0.4 mm space, 2x half layer height: 0.2 to 0.1 mm above & under.	pentagon in watch shape	5	3	3	3	yes	0/3
0.4 mm double walls + 0.7 mm space, 5x half layer height: 0.2 to 0.1 mm above & under.	pentagon in watch shape	5	3	-	3	only	2/3
<i>rectangles with two cubes</i>							
0.4 mm double walls + 0.7 mm space, 5x half layer height: 0.2 to 0.1 mm above & under.	rectangle with embedded cubes	4	5	-	1	only	1/2
0.4 mm double walls + 0.7 mm space, 5x half layer height: 0.2 to 0.1 mm above & under, 1mm cross sectional cut without walls in 1 plane, removed shell line: 2 to 1, fill:	rectangle with two cubes	4	5	-	1	only	2/4
0.4 mm double walls + 0.7 mm space, 4x half layer height: 0.2 to 0.1 mm above & under, 2mm cross sectional cut with walls in 2 planes, removed shell line: 2 to 1, changed fill honeycomb to grid.	rectangle with two cubes	4	5	-	1	only	2/3
0.4 mm double walls + 0.7 mm space, 4x half layer height: 0.2 to 0.1 mm above, under & middle, 2mm cross sectional cut with walls in 1 plane, removed shell line: 2 to 1, changed fill honeycomb to grid.	rectangle with two cubes	4	5	-	1	only	2/3
remarks:							
nozzle diameter is always 0.4, material is always PLA (jupiter series 123-3D), mostly white 2.85 mm, *= black 1.75mm, infill percentage mostly 10%, ^=15%							
All cubes were 30x30x30mm cubes, the round and octagonal tubes were 40 mm wide by 60mm tall, the triangles were 10 mm high and had even sides of 50 mm.							
In the test with the double walls, the Shred Result number is the amount of (almost) complete cubes that could be liberated in the shredder.							

APPENDIX VI: MICROSCOPE ANALYSIS OF LIBERATED SILVER TRACKS.

After silver tracks were liberated from samples (see page 36), the tracks were analysed with a microscope to verify whether the heat had decomposed the contact layer, or that the circuitry was loosened due to another reason.

As can be seen on the microscopy images in figure 70, a small trail in the substrate right under the circuit has melted, loosening the adhesion between PLA and silver. No PLA is left on the loose strings of silver, and no bits of silver stay attached to the molten substrate. Other samples show the effect of increased power dissipation: the PLA has locally disintegrated. Possible explanations for the spring-like movement of the silver are the thermal expansion of silver caused by the sudden rise in temperature, or stresses in the (silver) material caused by the drying after deposition being suddenly released when it detaches from the substrate. The cause of this behaviour was not further investigated.

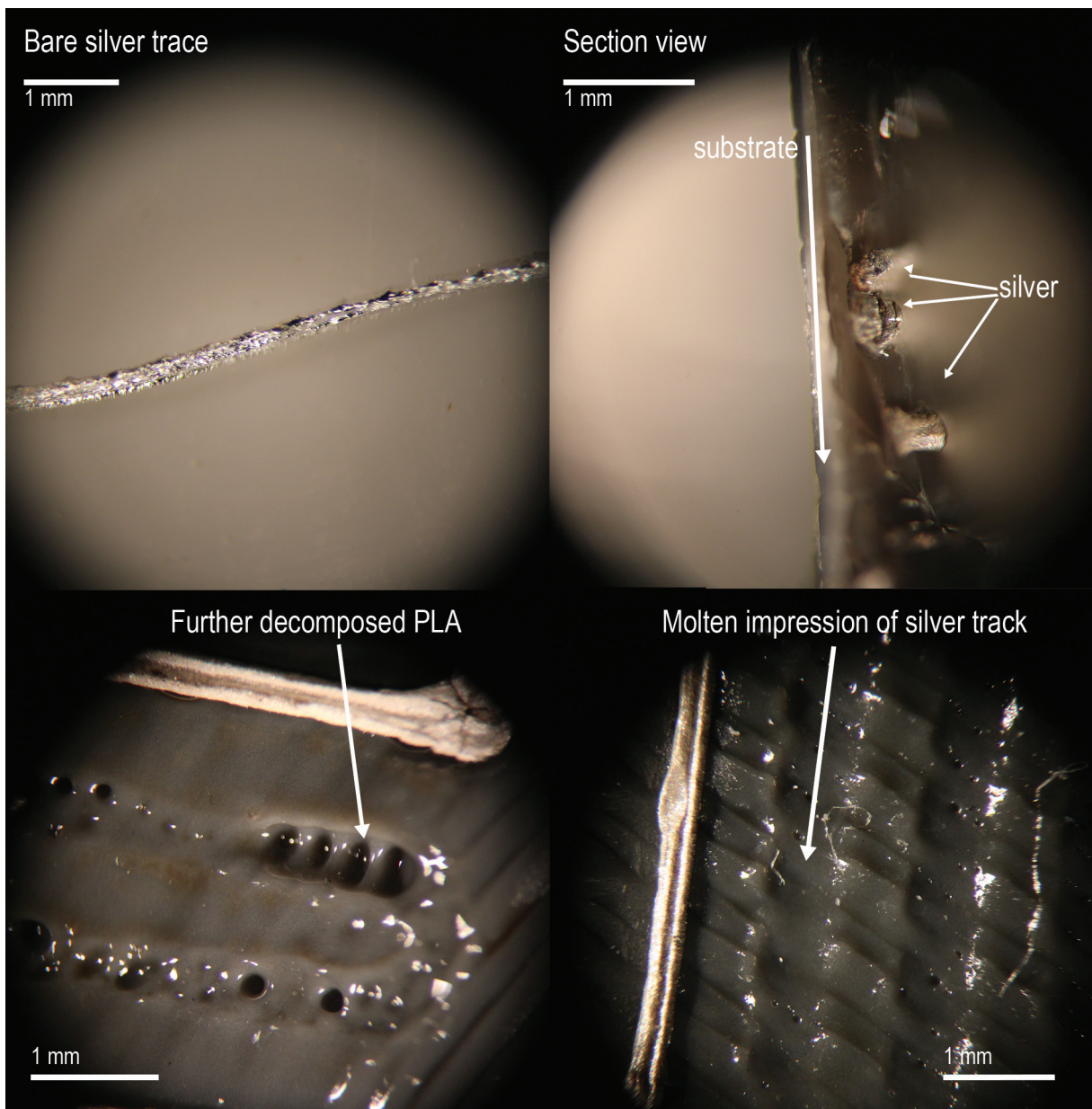


Figure 70: microscopy images of silver tracks and test samples.

The TU Delft logo is centered on the page. It features a stylized black flame icon above the letters 'TU' in a bold, black, sans-serif font, followed by the word 'Delft' in a lighter, blue, sans-serif font.

TUDelft

